AD-A032 136 ROCKWELL INTERNATIONAL THOUSAND OAKS CALIF SCIENCE --ETC F/G 11/6
STUDY OF INTERMETALLIC COMPOUNDS.(U)
JUN 76 C G RHODES, A G EVANS, N E PATON F33615-75-C-1090
UNCLASSIFIED AFML-TR-76-105 NL

| OF |
AD
A032136

END
DATE
FILMED
1-77

AFML-TR-76-105

12

B.S.

STUDY OF INTERMETALLIC COMPOUNDS

SCIENCE CENTER, ROCKWELL INTERNATIONAL
THOUSAND OAKS, CALIFORNIA 91360

JUNE 1976

TECHNICAL REPORT AFML-TR-76-105
FINAL REPORT FOR PERIOD FEBRUARY 1975 - FEBRUARY 1976

AIR FORCE MATERIALS LABORATORY
AIR FORCE WRIGHT AERONAUTICAL LABORATORIES
AIR FORCE SYSTEMS COMMAND
WRIGHT-PATTERSON AIR FORCE BASE, OHIO 45433

NOTICE

When Government drawings, specifications, or other data are used for any purpose other than in connection with a definitely related Government procurement operation, the United States Government thereby incurs no responsibility nor any obligation whatsoever; and the fact that the government may have formulated, furnished, or in any way supplied the said drawings, specifications, or other data, is not to be regarded by implication or otherwise as in any manner licensing the holder or any other person or corporation, or conveying any rights or permission to manufacture, use, or sell any patented invention that may in any way be related thereto.

This report has been reviewed by the Information Office (OI) and is releasable to the National Technical Information Service (NTIS). At NTIS, it will be available to the general public, including foreign nations.

This technical report has been reviewed and is approved for publication.

Harry A. Lipsitt

HARRY A. LIPSITT
Project Engineer

FOR THE COMMANDER

Norman M Tallan

NORMAN M. TALLAN
Acting Chief, Processing and
High Temperature Materials Branch
Metals and Ceramics Division
Air Force Materials Laboratory

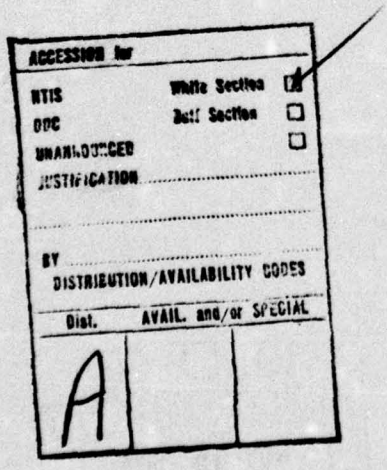

Copies of this report should not be returned unless return is required by security considerations, contractual obligations, or notice on a specific document.

(9) Final rept. 17 Feb 75–17 Feb 76,

Unclassified

SECURITY CLASSIFICATION OF THIS PAGE *(When Data Entered)*

REPORT DOCUMENTATION PAGE

READ INSTRUCTIONS BEFORE COMPLETING FORM

(18) (19) 1. REPORT NUMBER: AFML-TR-76-105

2. GOVT ACCESSION NO.

3. RECIPIENT'S CATALOG NUMBER

(6) 4. TITLE *(and Subtitle)*: Study of Intermetallic Compounds,

5. TYPE OF REPORT & PERIOD COVERED: Final Report 02/17/75 through 02/17/76

6. PERFORMING ORG. REPORT NUMBER: SC5022.5FR

(10) 7. AUTHOR(s): C. G. Rhodes, A. G. Evans, and N. E. Paton

(15) 8. CONTRACT OR GRANT NUMBER(s): F33615-75-C-1090

9. PERFORMING ORGANIZATION NAME AND ADDRESS: Science Center, Rockwell International, Thousand Oaks, CA

(16) 10. PROGRAM ELEMENT, PROJECT, TASK AREA & WORK UNIT NUMBERS: 7021, 702101, 61102F, 70210165 (17) 01

11. CONTROLLING OFFICE NAME AND ADDRESS: Air Force Materials Laboratory (LLM), Wright-Patterson AFB, Ohio 45433

(11) 12. REPORT DATE: June 1976

(12) 67p. 13. NUMBER OF PAGES: 64

14. MONITORING AGENCY NAME & ADDRESS *(if different from Controlling Office)*

15. SECURITY CLASS. *(of this report)*: Unclassified

15a. DECLASSIFICATION/DOWNGRADING SCHEDULE

16. DISTRIBUTION STATEMENT *(of this Report)*

Approved for public release; distribution unlimited

17. DISTRIBUTION STATEMENT *(of the abstract entered in Block 20, if different from Report)*

18. SUPPLEMENTARY NOTES

19. KEY WORDS *(Continue on reverse side if necessary and identify by block number)*

Titanium-Aluminum compounds, microstructure, mechanical properties

ALPHA 2

20. ABSTRACT *(Continue on reverse side if necessary and identify by block number)*

This report describes results of mechanical property tests and microstructure studies on a series of alloys based on the intermetallic compounds Ti_3Al (α_2) and TiAl (γ). This class of alloys has shown considerable promise for high temperature applications and the objective of this program has been to study the microstructure of a series of alloys containing both the α_2 and γ phases with a view to improving the mechanical properties. It has been shown that a variety of microstructures can be produced in a Ti-26% Al - 10% Nb base alloy, either by addition of ternary and quaternary alloying elements, or by heat treatment.

GAMMA

DD FORM 1 JAN 73 1473 EDITION OF 1 NOV 65 IS OBSOLETE

Unclassified

SECURITY CLASSIFICATION OF THIS PAGE *(When Data Entered)*

389 949

Aging of the alloys investigated resulted initially in precipitation of planar plates of γ phase in the α_2 matrix, followed by precipitation of a coarse $\alpha_2 + \gamma$ equilibrium microstructure resulting from a cellular reaction nucleated at the grain boundaries. The best fracture toughness and strength values were associated with the coarse $\alpha_2 + \gamma$ microstructure which formed either by overaging (as above) or with a coarse $\alpha_2 + \beta_2$ microstructure produced by solution treatment from the two phase region.

FORWARD

This Final Technical Report covers the work performed under Contract F33615-75-C-1090, Project No. 7021, from February 17, 1975 through February 17, 1976.

This contract with the Science Center, Rockwell International, Thousand Oaks, California was sponsored by the Air Force at Wright-Patterson Air Force Base, Ohio. It was administered under the technical direction of Dr. H. A. Lipsitt, Project Engineer, AFML/LLM.

The program was managed for Rockwell International by Dr. N. E. Paton. Mr. C. G. Rhodes had responsibility for the work performance under the contract. Dr. A. G. Evans provided technical assistance. Also providing experimental assistance at Rockwell International were Messrs. L. F. Nevarez, R. A. Spurling, P. Q. Sauers, E. H. Wright, and E. Charles.

TABLE OF CONTENTS

LIST OF ILLUSTRATIONS

I. INTRODUCTION

This is the final report on a research program to study the properties of alloys based on the titanium-aluminum system which show promise for high temperature applications. It is a part of a larger Air Force funded program with a number of participants working on various phases of an integrated effort to study the properties of a family of Ti-Al intermetallic compounds. The activities at the Science Center have been directed toward a careful study of the microstructure of a limited range of alloy compositions, to relate the observed microstructure to mechanical properties including high temperature strength, ductility and toughness.

The approach taken in this portion of the program has been to study the influence of alloying and heat treatment on microstructure of a series of alloys based on the composition Ti-26 wt pct Al - 10 wt pct Nb. This class of alloys generally has a microstructure consisting of an α_2 matrix with γ phase precipitates. It was felt at the outset of this program that an alloy based on a composition which could be heat treated to give a two phase microstructure would provide a better possibility of achieving the desired mechanical properties through control of the volume fraction and morphology of the second phase. This degree of freedom does not exist in a single phase system.

The intermetallic compounds based on the compositions Ti_3Al (α_2) and TiAl (γ) which form the binary Ti-Al alloys have been shown to have attractive elevated temperature strength and high modulus/density ratios but suffer from disastrously poor room temperature ductility.[1] The approach which has been adopted toward a

goal of improving ductility and toughness is to modify the microstructure by a combination of heat treatment to precipitate the γ phase in an alloy with an α_2 matrix, and by additions of ternary and quaternary elements.

The work is an extension of a company funded research program on α_2 type alloys which had been underway at the Science Center for about two years, and a brief description of the results of the latter program are to be found in the Background section of this report.

II. PROGRAM OBJECTIVES

The objective of the Air Force sponsored Titanium Aluminides Program was to select alloying additions for the compounds Ti_3Al, or TiAl, in order to improve room temperature ductility, elevated temperature creep strength, and/or elevated temperature oxidation resistance. The specific goals of the program for Ti_3Al base alloys were:

a) 2-4% elongation in tension at room temperature,

b) 100 hour stress rupture test: 40 ksi at 1400°F, with a minimum of 1% plastic strain,

c) oxidation resistance for use uncoated at 1400°F.

The studies conducted at the Rockwell International Science Center in connection with the Aluminides Program concentrated on alloys having the constitution $\alpha_2 + \gamma$. These studies utilized a base alloy composition, Ti-26 wt.pct. Al - 10 wt.pct. Nb (Ti-40 at.pct. Al - 4.5 at.pct. Nb), in which the γ-phase precipitates as plates. This base alloy was altered by various alloying additions aimed at increasing the misfit between α_2 and γ due to changes in the lattice parameters of one or both phases. Additionally, the effect of substituting Mo and/or V for Nb on the ordering kinetics of the α_2-phase was studied and the volume fraction γ-phase was determined as a function of Al content.

III. EXPERIMENTAL

All alloys reported on herein were prepared by standard arc melting techniques. The starting materials were electrolytic Ti sponge (El-60 grade) with a nominal purity of 99.8% and

Al - 99.999% pure
Nb - 99.98 "
V - 99.7 "
Mo - 99.7 "
Ni - 99.9 "
Cr - 99.99 "
Zr - 99.99 "
Cu - 99.999 "
Sn - 99.999 " .

The buttons were inverted and remelted a minimum of 10 times to ensure homogeneity. After melting, the buttons were wrapped in Ta foil, sealed in silica ampoules and homogenized at 1000°C for 1 week. The solutionizing and aging treatments were carried out in either an argon atmosphere or vacuum.

High temperature compressive flow stress determinations were made on extruded Ti-16 wt.pct. Al - 10 wt.pct. Nb and Ti-36 wt.pct. Al - 5 wt.pct. Nb samples cut from bar stock. These data were obtained for the purpose of estimating optimum forming parameters such as during rolling and forging. The determinations were made in a "Centorr" cold wall furnace with boron nitride lubrication on TZM platens. A tantalum face-sheet separated the sample from the TZM. This same equipment was used for upset forging of cast buttons prior to fabrication of tensile specimens. Flow stress was measured as a function of strain rate, with changes in strain rate being selected by the pushbutton crosshead speed control on the Instron machine used for testing. Strain rate was increased incrementally with sufficient time being given for a stable flow stress to be obtained at each crosshead speed.

The identification of phases present during the solution-temperature-determination phase of the study was accomplished by X-ray diffraction of polished surfaces. The analysis was performed using filtered CuK_α radiation and a Philips-Norelco diffractometer which was equipped with a graphite crystal, diffracted beam monochrometer to reduce the background due to Ti fluorescence.

A Philips EM-300 electron microscope equipped with a double-tilt goniometer stage was used to conduct the electron microscope observations. The thin foil samples were prepared using standard electropolishing techniques.[2]

Mechanical testing and indentation for fracture toughness estimates were performed on an Instron testing machine equipped with a furnace for elevated temperature testing. A strain gage extensometer was used to measure strain in the room temperature tensile tests.

IV. BACKGROUND

Since this work was an extension of a company funded research program on α_2 type alloys which had been underway at the Science Center for about two years, a brief description of the results of the latter program will be given in the following paragraphs, in order to provide the background for the research conducted under the subject program.

Binary Alloys

The elevated temperature strength of Ti-Al alloys containing 22, 25, 28, 31 and 34 at.pct. Al were measured between -196 and 830°C. The alloys all exhibit essentially no ductility in compression up to ~ 630°C. Thin foil electron microscopy examination of deformed specimens shows that the onset of ductility above 630°C is marked by the occurrence of $\bar{c}+\bar{a}$ slip and $\langle 10\bar{1}0\rangle$ (0001) slip. The latter was not observed at lower temperatures. Although this

observation could be ascribed to texture differences, this point has not been investigated.

One approach to limiting slip length and thus improving the ductility is the introduction of a small grain size by a martensitic reaction. Niobium additions to Ti-Al alloys which undergo a martensitic bcc $\rightarrow$ hcp transformation on quenching have been prepared and examined. The short slip length resulting from the small plate size, which is attainable, might mitigate brittleness. The addition of Nb also results in a marked decrease in ordering kinetics, with ordering completely suppressed during quenching in a Ti-25 at.pct. Al - 4.8 at.pct. Nb alloy. This ability to suppress the ordering reaction permits increased ductility for an intermediate forming step after which elevated temperature strength can be restored by low temperature aging to produce long range order. Preliminary mechanical property measurements on these alloys show significant improvements in both strength and ductility compared to Ti_3Al. The major problem with these alloys is the occurrence of an in-situ recrystallization process which tends to re-coarsen the grain size during elevated temperature exposure.

$\alpha_2 + \gamma$ Alloys

Alloys with sufficiently high Al content to allow precipitation of γ-phase in the α_2 matrix is another system which has the potential for forming precipitates which can limit slip lengths. Preliminary mechanical property measurements on a Ti-26 wt.pct. Al - 10 wt.pct. Nb aged alloy indicated significant increases in yield strengths compared to single-phase alloys.

The γ-phase in these alloys precipitates as long plates with $(0002)\alpha_2 \parallel (111)\gamma \parallel$ interface and $[11\bar{2}0]\alpha_2 \parallel [011]\gamma$, Figure 1. The plates extend across each grain resulting in a quasi-layered structure of α_2 and γ. The planar interphase boundaries may well be a source of premature failure by providing

both crack nucleation sites (due to stresses built up by the non-transfer of slip from α_2 into γ plate) and crack propagation paths. Therefore, an equiaxed precipitate morphology may be more effective in raising room temperature ductility. Equiaxed particles are present at grain boundaries in the aged condition, indicating that thermomechanical processing might be employed to produce equiaxed γ particles.

V. RESULTS

Selection of Alloys

The alloys selected for study are listed in Table I. Alloy 0 has the base alloy composition and each of the others is a variation of that alloy. As indicated in the Background section, the room temperature ductility might be improved by altering the precipitate morphology or by decreasing the degree of order in the Ti_3Al matrix. The alloying additions were selected for their possible influence on these parameters. In Alloys 1-4, vanadium or molybdenum was substituted for niobium to determine the effect of each of these on the degree of order

The γ-phase grows as plates because of the orientation relation and the low misfit between γ and α_2 phases along the (0001) α_2 and $(111)\gamma$ habit plane. Room temperature ductility might be expected to be further increased by the presence of more equiaxed precipitates, which may be produced by changing the lattice parameters, hence misfit, of the α_2 and/or γ phases. Alloys 5-11 and 17-19 were selected to change the lattice parameters by substituting Cr, Ni, or Sn for Al and Zr for Ti.

Since the nucleation and longitudinal growth of the γ phase has been suggested to result from the dissociation of a 1/3 $\langle 11\bar{2}0\rangle$ α_2 dislocation into 1/3 $\langle 10\bar{1}0\rangle$ partials generating long ribbons of γ phase,[3] increasing the energy of formation of 1/3 $\langle 10\bar{1}0\rangle$ partials by increasing the stacking fault

energy may alter the morphology of the γ-phase precipitates. Alloy 12 was selected because Cu decreases the electron concentration, (e/a), when substituted for Al.

The strength and ductility of the $\alpha_2 + \gamma$ alloy also may depend on the relative amounts of each phase present. Therefore, Alloys 13-16 were selected to determine volume fraction γ phase as a function of Al content, and Alloys 23-26 were prepared to determine the effect of Al content on tensile properties.

Microstructural Evaluation

A. Base Alloy

Figure 2 is the Ti-Al binary phase diagram published in Metals Handbook.[4] Although this diagram may be open to some question regarding detailed phase boundary positions, it was useful as a guideline for the present work. The base alloy, Ti-26 wt.pct Al - 10 wt.pct. Nb, was solution-treated in the single-phase α_2 region at 1250°C and quenched. Subsequent aging in the $\alpha_2 + \gamma$ field at 800°C produced structures such as that in Figure 1.

The aging treatments were conducted at 700, 800, 900 and 1000°C. The results showed that the initial morphology of the γ-phase precipitate was plate-like, as illustrated in Fig. 1, at all temperatures. In addition to this intragranular precipitation, there is also a cellular reaction, $\alpha_2 \rightarrow \alpha_2 + \gamma$, which nucleates at grain boundaries and grows at a much slower rate than the intragranular reaction. As a result, the cellular reaction, which produces a coarse dispersion of γ in α_2, consumes the fine dispersion of intragranular $\alpha_2 + \gamma$ as it grows into the grain interiors, Fig. 3. The kinetics of γ-phase precipitation, which are summarized in Table II, increased rapidly with temperature over the range examined. 800°C was selected as the standard aging temperature for several reasons. Firstly, it is above the program maximum-temperature objective of 760°C (1400°F), thereby minimizing stability problems during high temperature

testing (and operation). Also 800°C aging allows convenient control of the microstructure, wherein aging for 4 or 6 hours produces only intragranular γ-phase, aging for 8 hours initiates the cellular reaction, and continued aging produces increasing amounts of coarse $\alpha_2 + \gamma$.

Since our basic goal was to develop $\alpha_2 + \gamma$ structures, the approach for each of the alloys was to determine the appropriate solution temperature to produce a supersaturated single phase α_2 structure which would then be amenable to aging. In this work where a large number of alloy compositions is being examined, the clearest, most concise manner in which to present the results appears to be in groups according to the function of the alloying additions as described in the previous section.

B. Substitution for Niobium

Figures 4 through 7 are light micrographs of microstructures of Alloys 1-4. The partial substitution of V for Nb (Alloy 1) resulted in a lowering of the solution temperature to 1150°C. However, the full substitution of V for Nb (Alloy 2) expanded the β-phase region (see Fig. 2) so that solution treating at temperatures from 1150 to 1300°C resulted in some β-phase being present in the α_2 matrix, Fig. 5.

The substitution of 3.6 wt.pct. Mo for Nb (Alloy 3) resulted in an alteration of the α_2 morphology. Solution treating in the temperature range of 1150 to 1300°C produced lath-like α_2 dispersed in a β matrix, Fig. 6. When 7 wt.pct. Mo was added in place of the Nb (Alloy 4), the β-phase field expanded such that 1300°C was within the single-phase β field while the two phase, $\alpha_2 + \beta$, field encompassed the 1150 to 1250°C temperature range, Fig. 7. It is of interest to note that the retained β-phase in all alloys is ordered having either the CsCℓ (B2) or the Heusler ($L2_1$) structure, and, as such, will hereafter be designated β_2.

Measurements of long range order parameters in these alloys were not attempted in this program. Rather, the effects of Mo and V substitutions were evaluated by the relative changes in hardness measurements and tensile tests. Since these alloys were not designed to produce a change in γ-phase precipitate morphology, extensive aging experiments were not conducted.

C. Substitution for Al

The partial substitution of Ni for Al (Alloys 5, 5A, 6, 7) resulted in a shift of the β-phase field so that a two, or three, phase field extended through the 1150 to 1225°C temperature range. The single-phase β_2 field was found to exist at 1300°C for Alloy 5A, the lowest Ni bearing alloy with 1.4 wt.pct. Ni. The β_2 field appeared to be lowered with increasing Ni content, being 1250°C for Alloy 7.

Although the single-phase α_2 region was not attained for Alloy 5A, treatment at 1175°C produced a large volume fraction of lath-like α_2 in a β_2 matrix, Fig. 8. This structure was then aged to determine the effects of Ni on the γ-phase precipitate morphology. Aging for 4 hours at 800°C revealed no change in the γ-phase morphology, Fig. 9a. The β_2 phase also partially decomposed during the aging treatment to a mixture of α_2 and Ti_2Ni in the β_2 matrix, Fig. 9b.

Alloy 7 was also aged at 800°C in the retained β_2 condition. Fine α_2 laths were precipitated throughout the β_2 matrix in addition to small faulted particles of Ti_2Ni, Fig. 10.

The partial substitution of Cr for Al (Alloy 8, 8A, 9) produced a result similar to that described for the Ni substitution. A single-phase α_2 region was not detected for these alloys with a two phase, $\alpha_2 + \beta_2$, field found to exist over the temperature range of 1150 to 1250°C. For the alloys containing the larger amounts of Cr (Alloys 8 and 9) the single-phase β_2 region existed at 1300°C.

Treatment of Alloy 8A at 1175°C produced a large volume fraction of lath-like α_2 with a small amount of retained β_2. The β_2 was found to contain ω-phase in the as solution treated condition, Fig. 11. Aging this structure at 800°C produced γ-phase in the α_2 laths in the familiar plate-like morphology; the omega phase particles in the β_2 phase have coarsened, not reverted, during the 800°C exposure. The single-phase β_2 in Alloys 8 and 9 decomposes by the precipitation of α_2 particles during 800°C aging, Fig. 12.

Alloy 12, which has 2.1 wt.pct. Cu as partial substitution for Al and no Nb, could be solution treated at 1150°C to produce a single phase α_2 structure. Subsequent aging at 800°C indicated the morphology of the γ-phase was not altered by the presence of Cu.

When Sn was added as partial substitution for Al in Alloys 17, 18 and 19, the solution temperature was not altered from 1250°C. The morphology of the γ-phase formed during subsequent 800°C aging was similar to that observed in the base alloy and each of the previously described alloys, i.e. plate-shaped precipitates extending across the α_2 grains.

D. Substitution for Ti

The results on Alloys 10 and 11 were somewhat enigmatic in that the lower Zr addition (Alloy 10) exhibited a two phase field ($\beta_2 + \alpha_2$) from 1150°C up through 1250°C and a single-phase β_2 field at 1300°C, whereas the higher Zr containing alloy (11) exhibited a single-phase α_2 structure after treatment at 1300°C.

The ordered β-phase in Alloy 10 contained ω-phase after quenching, as indicated in the selected area electron diffraction pattern of a [113] β_2 zone, Fig. 13. The particles were too fine to image by dark-field techniques. However, the ω-phase particles grew during low-temperature aging, as illustrated in Fig. 14.

E. Summary of Microstructures

The solution temperature determinations aimed at producing single phase, supersaturated α_2 in Alloys 1-12 and 17-19 resulted in either single phase α_2 or single phase β_2, or a mixture of the two. The behavior of the alloys can be understood if one considers the ternary and quaternary alloys as pseudo-binary alloys which can be described by the phase diagram in Fig. 2. For instance, those alloys in which Al was substituted for by Ni or Cr have an effective Al content lower than the base alloy and would be expected to have the β-phase field existing at a lower temperature which indeed is observed. In those alloys in which Mo or V was substituted for Nb, the actual position of the β-phase field has been shifted to the left (in Fig. 2) resulting in a lower β transus for each composition. Similarly, if the shape of the β-phase field is altered slightly by the alloying addition to a more nearly vertical position over the temperature range of interest (1150 - 1300°C) the two-phase, $\alpha_2 + \beta_2$, field would be unavoidable during solution treatment.

Although the alloying additions have not altered the morphology of the γ-phase precipitate particles, the growth kinetics were modified. For instance, aging at 800°C for 4 hours produces ~ 30% γ-phase in Alloy 1, whereas Alloy 11 has 65% and Alloy 12 has 45% γ-phase present. The base alloy has about 30% γ-phase after 4 hours at 800°C. The aging treatment at 800°C also has some effect on the ordered domain size in the α_2 matrix. The domain size in the solutionized base alloy is on the order of 1000 Å and after 8 hours at 800°C the domain have grown to approximately 2000 Å, Fig. 15. In Alloy 12 the domain sizes are approximately equivalent to those in the base alloy, but in Alloy 11 the domains are significantly smaller, as illustrated in Fig. 16.

The results of this portion of the program have shown that a variety of microstructures can be produced in the various alloys. Examples of the

different solution treated conditions which can be generated are: (1) single phase, equiax grained α_2, (2) single phase, equiax grained β_2, (3) equiax grained α_2 with retained β_2, and (4) α_2 laths (in varying amounts) in β_2 matrix. Each of these structures can then be aged to precipitate γ-phase in the α_2 and α_2 phase in the β_2.

Volume Fraction γ-Phase Determination

The strength and ductility of the two phase, $\alpha_2 + \gamma$, alloys will be affected by the relative amounts of the phases present in the microstructure. Therefore a determination of the volume fraction γ-phase as a function of Al content was performed to ascertain if the addition of Nb shifted the phase boundaries as described by the phase diagram, Fig. 2. The four alloy compositions which were evaluated are Ti-10 wt.pct. Nb with additions of 23.3, 28.4, 28.5, and 30.9 wt. pct. Al (analyzed values). Samples were solution treated and aged at 800°C or 900°C for 24 hours. Volume fraction of γ-phase was not a function of temperature, within experimental error, for the 23.3 and 28.4 wt.pct. Al alloys indicating that, assuming the phase boundaries are parallel in this temperature range and precipitation kinetics are increased with increasing aging temperature, equilibrium had been reached. The results for the four alloys aged at 800°C for 24 hours are plotted in Fig. 17. The dashed line in the figure is the equilibrium value predicted by the Ti-Al binary phase diagram in Fig. 2. The results indicate that the α_2 and γ-phase boundaries at 800°C have not been shifted significantly by the 10 wt.pct. Nb addition.

Flow Stress Measurements

Flow stresses of Ti-16 wt.pct. Al - 10 wt.pct. Nb and Ti-36 wt.pct Al - 5 wt.pct. Nb powder extrusions were determined in compression as described in the experimental section. The results are shown in Figs. 18 and 19 with the

actual data listed in Table III. Also shown in Table III are the maximum strain rate sensitivities, m (m= ∂ log stress/∂ log strain rate) obtained during each test. The high values of m indicated are evidence that these materials are probably suitable for superplastic forming and isothermal forging.

Thermomechanical Processing

Solution-treated samples of the base alloy, Ti-26 wt.pct Al - 10 wt.pct. Nb, were deformed in compression approximately 10% at 700°C, 800°C, and 900°C. As indicated in the Background section, it was anticipated that the introduction of a high density of dislocations in the α_2 prior to aging could alter the γ-phase precipitate morphology.

Aging of the deformed specimens at 800°C produced the familiar plate morphology of the γ-phase. It appears quite likely that a sufficiently high dislocation density to significantly alter the precipitate morphology is unattainable in this alloy.

Fracture Toughness Estimates

Approximate values for the critical stress intensity factor, K_c, were determined using a recently developed indentation technique.[5] The technique requires that a strain-free, polished surface of the material (e.g. an electrolytically polished surface) be indented, using a Vicker's indenter, to a load level which causes radial cracks to develop from the corners of the indentation. Then measurements of the load, P, the indent diagonal, 2a, and the radial crack length, C, permit a direct estimation of the fracture toughness, using the unique relation between the normalized crack length, C/a, and the normalized fracture toughness, $K_c\Phi/H\sqrt{a}$ (where H is the hardness and Φ is the constraint factor), as shown in Fig. 20.

Initially, two aluminides (solution treated and precipitation hardened samples of Alloy O) were tested in the prescribed manner, to assess the utility of the indentation technique. Cracks were induced in both materials, at loads $\gtrsim$ 500 N. However, the normalized crack lengths, C/a ~ 0.1 to 0.2, were at the upper extreme of the calibration curve (Fig. 20), and the absolute error in the K_c measurement could thus be substantial (up to 30%), although the relative error should be small. Based on the results of these two samples, it was decided to use the technique to rank eleven selected alloy compositions. The alloys were evaluated, in most instances, in both the solutionized and aged conditions. In several cases no cracks were present after indentation with the maximum available load. Since calculations showed that cracks would have formed in these materials if K_c were <12 ksi$\sqrt{in}$, these non-cracked samples are grouped together under the designation K_c > 12 ksi$\sqrt{in}$. The measured toughness values are presented in Table IV; in addition the flow stress at 8% strain estimated from hardness values, and the microstructural characteristics are included in the table. It can be seen that there is a very good correlation of estimated K_c with microstructure. Micrographs of typical examples of these various microstructures are presented in Figures 21-24.

Although the precise relationship of these estimated K_c values to actual fracture toughness values has not been determined, the correlation of microstructure to the estimated values is very encouraging. It is therefore quite likely that the hierarchy of results is an acceptable method of rating samples. The following tentative conclusions may thus be drawn from the results:

1) A coarse, two-phase structure, consisting of either $\alpha_2 + \beta_2$ or $\alpha_2 + \gamma$, is superior to the single phase α_2 or the typical planar γ-phase precipitation in α_2 in terms of both toughness and yield strength;

2) The typical planar precipitation of γ-phase in an α_2 matrix improves the toughness and yield strength over the single phase α_2 structure.

A further breakdown of the tested samples into groups according to the function of the appropriate alloying addition is given in Table V. In the first group, it can be seen that substituting Mo for Nb clearly improves both the toughness and the yield strength in the aged condition, while substituting V for Nb has little effect on these properties. In the second group, the toughness and yield strength are improved when Cr is substituted for Al, whereas Ni substitution does not influence these properties. As indicated earlier, the mechanism for improving the toughness and yield strength by the Mo substitution and the Cr substitution is the alteration of the microstructure of the "solution-treated" condition from single-phase, equiax grained α_2 to a two-phase structure consisting of coarse α_2 particles in a β (or β_2) matrix.

The Zr substitution for Ti in the third group also resulted in an increase in toughness which could be attributed to a coarse, two-phase microstructure. In this instance, there was a coarse dispersion of γ-phase in the α_2 matrix. The Cu and Sn substitutions for Al had no effect on γ-phase morphology and consequently little effect on toughness or yield strength.

The final group reflects the influence of volume fraction γ-phase on toughness and yield strength. Again, the higher Al content resulted in a "solution-treated" microstructure of a coarse dispersion of γ-phase in an α_2 matrix producing the higher toughness values.

Tensile Testing, Room Temperature

Five alloys were selected for tensile testing based on the results of the estimated fracture toughness measurements. These were Alloys 1, 3, 4, 8A and 11 which span the range of estimated K_c and flaw stress values, as well as being representative of the various microstructures attainable in these alloys,

Table IV. In addition, the base composition, Alloy 0, was selected, as were Alloys 23 and 26, in which the volume fraction γ-phase is varied. A Ti-26 wt.pct. Al - 7.5 wt.pct. Nb powder extrusion (6219-A) obtained from ARL was also included in the tensile testing.

Tensile samples were form ground from material which had been hot pressed from 1.5" long by 0.5" diameter loaf buttons to 0.25" thick pancake forgings. A drawing of the tensile sample configuration is shown in Fig. 25 and the TZM grips in Fig. 26. Hot pressing was performed at temperatures $\geqslant$ 1200°C for all alloys. Light microscopy of the alloys prior to grinding indicated that microcracks were limited to within 10 mils of the surface and no pores or cracks were apparent in the interiors of the forgings.

For the first series of tests, the gauge length of each of the tensile specimens was electropolished prior to testing in order to minimize surface cracks which can initiate premature failure. The specimens were examined for cracks after electropolishing and it was found that surface cracks existed in the gauge section even after the removal of approximately 4 mils. The number and degree of cracks varied from sample to sample. The amount of electropolishing that could be applied to the samples was limited because of the nonuniform attack in the vicinity of the shoulder of the tensile specimen which mates to the grip and carries the load during testing. A comparison of the results of polished and non-polished tensile specimens indicated no improvement due to electropolishing and therefore all subsequent samples were not electropolished prior to testing.

The room temperature tests were performed at a strain rate of either 2.2 or 4.5×10^{-4} sec^{-1}. The results are presented in Table VI. All of the alloys show fracture stresses considerably below that expected for Ti_3Al[6] or that predicted by the indentation technique, Table IV. Approximately one-half of

the samples tested fractured in the shoulder which may indicate stress concentrations in this portion of the sample during loading. Alternatively, the premature failure of the samples may be the result of surface cracks which could not be completely eliminated by electropolishing.

Since the samples have failed prematurely, meaningful evaluations of the effects of microstructure on tensile properties cannot be made. However, fractography does provide some insights as to the influence of microstructure on fracture modes. The effect of the γ-phase precipitates on the fracture topography is illustrated in Figs. 27 and 28. The fracture in the solutionized condition is a smooth cleavage typical of a low-energy, brittle failure. The presence of the γ-phase precipitates has rendered the fracture path more tortuous, indicative of a higher fracture energy, which has been shown to correlate positively with fracture toughness[7] and is consistent with the indirectly measured K_c values reported in Table IV.

Alloy 1 exhibited a yield point indicative of some plasticity when aged for 4 hours at 800°C. The microstructure of this sample consisted of a fine grained ($\sim$ 50 μm diameter) α_2 matrix with intragranular planar γ-phase and intergranular retained β-phase, Fig. 29a. Fractography revealed a mixed transgranular and intergranular fracture mode, Fig. 29b, indicating the presence of β-phase at the grain boundaries promotes intergranular failure. It is quite likely that the observed ductility results from the smaller grain size that this sample exhibited. (Alloy 0, for instance, had an α_2 grain size of approximately 100 μm.)

Alloys 3 and 4 in the solution-treated condition were composed of acicular α_2 plates in β_2 matrix and Alloy 8A had coarse α_2 particles in retained β_2 matrix. Fractography of these samples reveals that the fracture mode is cleavage of the individual α_2 plates with the increased strength (over single-phase α_2 as indicated by Table IV) resulting from the increased energy necessary to pass the crack through the β_2 phase to link up the cleavage cracks.

Alloy 11 was solutionized at 1285°C producing single phase β_2, in which the fracture mode was cleavage, similar to the α_2 fracture mode. The aged microstructure consisted of a fine dispersion of α_2 in β_2, which did not alter the cleavage fracture mode, but provided barriers to the advancing cleavage crack resulting in a rough fracture surface.

The results from Alloys 23 and 26 indicate that a larger volume fraction of γ-phase produces a higher fracture stress. The Alloy 26 sample aged 48 hours at 800°C exhibited a yield point; similar to the Alloy 1 sample, this particular sample had an α_2 grain size on the order of 50 μm.

Compression Testing, Elevated Temperature

Elevated temperature compression testing was performed on selected samples. Solution treated and aged specimens of Alloys 1, 8A, 11, and 12 were tested at 600°C and 800°C. As was the case for the tensile samples, the aging treatment of 4 hours at 800°C was selected for the compression samples. The results are presented in Fig. 30, in which are also plotted the data for the base alloy and stoichiometric Ti_3Al, which were determined at the Science Center previously.

Alloys 1, 11 and 12 had the same basic microstructure consisting of large α_2 grains containing planar γ-phase precipitates, as was illustrated in Fig. 1. The alloys show a considerable strength increase over stoichiometric α_2 and over the solution treated base alloy. The high strength of Alloy 8A is attributable to the α_2 lath morphology.

Tensile Testing, 1400°F (760°C)

Samples of the alloys tensile tested at room temperature were also tensile tested at 1400°F (760°C) in air. The results are listed in Table VII. Of the group, only Alloy 8A (Ti-25.2 wt.pct Al - 1.2 wt.pct Cr - 10 wt.pct Nb) exhibited a yield point indicating significant plasticity. Elongation, determined by measurement of the sample after fracture, was found to be approximately 2% as

solutionized and 1.5% as aged. This alloy also showed promise in the indentation tests and the room temperature tensile tests.

The other alloys tested, including the base alloy, showed no significant difference in tensile behavior at 1400°F as compared to room temperature. That is, the fracture mode at 1400°F was virtually identical to that observed at room temperature for each of the alloys. The very brittle nature of the fractures at 1400°F would indicate that the ductile-brittle transition is above 1400°F for these alloys, contrary to what others have observed,[6] and may be a consequence of the difference in processing procedures used. The alloys tested here were cast and hot pressed, whereas others have tested material produced by a powder processing and extrusion technique.

VI. DISCUSSION

The results of this study have shown that substituting Cr, Ni, or Sn in moderate amounts for Al in Ti-26 wt.pct. Al - 10 wt.pct. Nb may alter phase boundaries and introduce additional phases into the microstructure, but does not influence the mechanism, and hence the particle morphology, of γ-phase precipitation from the supersaturated α_2 phase. The initial intragranular precipitation of γ-phase as plates on the order of 300-500 Å in width is not the equilibrium structure for these two phase, $\alpha_2 + \gamma$, alloys. The cellular reaction, which is more sluggish than the intragranular precipitation, eventually occurs and, with time, consumes entirely the fine $\alpha_2 + \gamma$ mixture, replacing it with a coarse (3000-5000 Å separation) $\alpha_2 + \gamma$ mixture. The various alloying additions studied in this program have not altered this basic precipitation mechanism.

The microstructure was, however, manipulable in terms of the α_2 phase. Several of the alloys could be solution treated in the two-phase, $\alpha+\beta$, field, in which varying volume fractions of α_2 lath-like particles were attained.

The β-phase, which was retained during quenching or air cooling, generally had the ordered bcc structure. In this series of alloy compositions, a Widmanstätten α structure which sometimes forms from the β-phase during slow cooling was not obtained during air cooling. That is, the alloys generally were too rich in β stabilizers to transform either martensitically during a quench or by nucleation and growth during air cooling. The α_2 morphology, then, could be manipulated only by heat treating in the α+β phase field.

In several of the alloys, the β_2 phase, which was retained after a water quench, contained omega phase. The presence of ω-phase in an ordered structure was somewhat surprising in view of the displacement controlled reaction theory of ω-phase formation proposed by de Fontaine.[8] This theory explains the diffuse intensity distribution (streaking), which generally precedes omega formation, observed in electron diffraction patterns as resulting from random or uncorrelated displacements of atoms in the bcc lattice. It would seem that such displacements would degrade the ordered bcc structure along with omega phase formation. Future refinements of omega formation theories will have to account for its presence in ordered as well as disordered matrices.

Of the various techniques used in this program to measure the effects of microstructure on mechanical properties, the indentation technique was the most fruitful. The correlations of the indentation data with microstructure which were described in the Results section are good evidence of the utility of this technique. The microstructure which gave the best results in terms of estimated K_c and flow stress was a coarse mixture of α_2 and γ or coarse α_2 particles in a β_2 matrix. The coarse $\alpha_2 + \gamma$ mixture was an as-cast structure which had not been subsequently refined. The cellular reaction which nucleates at grain boundaries and grows into the grains creates a coarse α_2 plus γ structure, indicating that aging hot-pressed material for long times would not only produce a more stable microstructure, but quite possibly, one with better mechanical properties.

The indentation technique also has confirmed that the two-phase microstructure of fine planar γ phase in an α_2-phase matrix improves the strength over the single-phase α_2 structure. The improved properties of alloys having a microstructure consisting of lath-like α_2 particles in a β_2 matrix are a result of the reduced slip length within each α_2 "grain" as described in the Background section.

Room-temperature tensile ductility was observed in samples having a grain size on the order of 50 μm, whereas no ductility was evident for identical microstructures with grain sizes on the order of 100 μm or larger. This result is in agreement with the hypothesis of reduced slip length improving ductility presented in the Background section. The anomalous fine-grained samples were subjected to the same thermal processing (arc melting, hot-pressing, solutionizing, and aging) as all other samples. The source of the reduced grain size may lie with variations in conditions along the 6" loaf button during arc-melting.

Tensile test results generally showed premature failure as well as no measurable plasticity. Although brittle materials, which are extremely sensitive to surface flaws, frequently fail prematurely during tensile testing, most of the elevated temperature tests also showed no measurable plasticity, indicating the tests have not been a good absolute measure of the properties. This condition arose because of the restricted size of the tensile samples resulting from the limited size of the hot-pressed pancake.

The elevated temperature compression tests showed that high temperature strength is improved by the precipitation of γ-phase in the α_2-phase matrix. The results of these tests when viewed along with the indentation technique results show that the strength of the single phase α_2 can be significantly improved from room temperature up to 900°C by aging to produce a two-phase $\alpha_2 + \gamma$ structure.

VII. CONCLUSIONS

1. A variety of microstructures can be produced in $\alpha_2 + \gamma$ alloys by varying the base alloy composition of Ti-26 wt.pct. Al - 10 wt.pct. Nb.
2. A microstructure with coarse α_2 particles can be produced by solution treatment of certain modifications of the base alloy in the two phase $\alpha_2 + \beta$ region.
3. The planar morphology of γ-phase produced on aging is not readily altered by minor substitutions of Ni, Cr, Sn, Cu or Zr.
4. The cellular reaction, $\alpha_2 \rightarrow \alpha_2 + \gamma$, initiates at grain boundaries and supersedes the intragranular precipitation of γ-phase, thereby producing a coarse $\alpha_2 + \gamma$ structure as the equilibrium microstructure.
5. Positive correlation of microstructure with an indentation method for measuring toughness indicates this to be an effective technique for the relative ranking of microstructures in terms of fracture toughness and flow stress.
6. Indentation-technique results show that the fracture toughness and flow stress of single phase α_2 can be improved by the precipitation of planar γ-phase. The best fracture toughness and strength values are associated with a microstructure consisting of coarse $\alpha_2 + \gamma$ or coarse α_2 particles in a β_2 matrix.

VIII. REFERENCES

1. M. J. Blackburn and J. C. Williams, Trans. ASM, Vol. 62, (1969) pp. 398-409.
2. R. A. Spurling, Met. Trans., Vol. 6A (1975) pp. 1660-61.

3. M. J. Blackburn, "The Science, Technology and Application of Ti," R. I. Jaffee and N. E. Promisel, eds., Pergamon Press, Oxford, 1970, pp. 633-43.

4. "Metals Handbook," 8th Ed., Vol. 8, 1973, ASM, Metals Park, Ohio, p. 264

5. A. G. Evans, "Quasi-Static Solid Particle Damage in Brittle Solids-II. Implications," to be published, Acta Met.

6. R. Schafrik, "Mechanical Properties and Deformation of Ti_3Al at Elevated Temperatures," ARL (AFSC) Project 70210138, 2nd Quarterly Report, 1975.

7. R. G. Berryman, F. H. Froes, J. C. Chesnutt, C. G. Rhodes, J. C. Williams, and R. F. Malone, "High Toughness Alloy Development," Contract N00019-75-C-0335, Final Report, TFD-74-637, July 1974.

8. D. De Fontaine, Acta Met., Vol. 18 (1970) pp. 275-79.

TABLE I

ALLOYS FOR ALUMINIDES PROGRAM

Nominal Compositions in at.pct (wt.pct.)

Alloy	Ti	Al	Nb	V	Mo	Ni	Cr	Zr	Cu
0	Bal	40 (26.6)	4.5 (10)						
1	"	40 (26.6)	2.3 (5.3)	2.3 (2.9)					
2	"	40 (27.2)		4.5 (5.8)					
3	"	40 (26.8)			1.5 (3.6)				
4	"	40 (26.3)			3.0 (7.0)				
5	"	32.5 (20.2)	4.5 (9.6)			2.5 (3.4)			
5a	"	39 (25.1)	4.5 (10.0)			1.0 (1.4)			
6	"	35 (21.9)	4.5 (9.7)			5.0 (6.8)			
7	"	30 (18.1)	4.5 (9.3)			10.0 (13.1)			
8	"	35 (22)	4.5 (9.8)				5 (6.1)		
8a	"	39 (25.2)	4.5 (10.0)				1.0 (1.2)		
9	"	30 (18.4)	4.5 (9.5)				10.0 (11.8)		
10	"	40 (24.7)	4.5 (9.6)					5 (10.4)	
11	"	40 (23.5)	4.5 (9.1)					10 (19.9)	
12	"	39.4 (26.7)							1.3 (2.1)
13	"	35.5 (22.5)	4.6 (10)						
15	"	42.5 (27.9)	4.5 (10.2)						
16	"	45 (30.0)	4.5 (10.3)						

TABLE I - (Continued)

ALLOYS FOR ALUMINIDES PROGRAM

Nominal Compositions in at.pct (wt.pct.)

Alloy	Ti	Al	Nb	Sn
17	Bal	39 (24.8)	4.5 (9.8)	1.0 (2.8)
18	"	38 (23.6)	4.5 (9.6)	2.0 (5.5)
19	"	35 (20.5)	4.5 (9.1)	5.0 (12.8)
23	"	39 (25.2)	4.5 (10.0)	
24	"	41 (26.8)	4.5 (10.1)	
25	"	43 (28.3)	4.5 (10.2)	
26	"	44 (29.1)	4.3 (9.9)	

TABLE II

SUMMARY OF γ-PHASE PRECIPITATION KINETICS

IN Ti-26 WT.PCT. Al - 10 WT.PCT. Nb

Temperature	Initial Observation of Intragranular γ	Initial Observation of Cellular Reaction
700°C	8 hrs	> 8 hrs
800°C	2 hrs	8 hrs
900°C	½ hr*	½ hr*
1000°C	½ hr*	½ hr*

* did not examine for shorter times

TABLE III

FLOW STRESS MEASUREMENTS OF POWDER EXTRUSIONS

	16Al-10Nb Stress (ksi)			Ti-36Al-5Nb Stress (ksi)			
$\dot{\varepsilon}$ (sec^{-1})	1550F (843C)	1700F (927C)	1900F (1038C)	1700F (927C)	1900F (1038C)	2100F (1149C)	2400F (1316C)
5.32×10^{-5}	47.43	37.08	10.35	24.54	6.98	3.49	1.45
1.33×10^{-4}	53.22	40.27	12.74	28.15	10.73	4.44	2.39
2.66×10^{-4}	60.26	44.20	14.92	31.76	13.07	5.50	3.01
5.32×10^{-4}	72.60	50.09	17.21	36.57	15.80	7.08	3.59
1.33×10^{-3}	79.38	57.85	20.39	44.27	20.39	9.76	
2.66×10^{-3}	85.18	63.75	23.88		24.87		
m (max)	.25	.17		120	.45	.359	.69

TABLE IV

ESTIMATES OF FRACTURE TOUGHNESS AND FLOW STRESS (AT 8% STRAIN)

Alloy Designation	Condition	K_c (ksi$\sqrt{in}$)	σ (ksi)	Microstructure
8A	S.T. + 800°C/8hrs/AC	> 12	215	Coarse acicular α_2 containing planar γ
4	S.T. + 800°C/8hrs/AC	> 12	196	Coarse α_2 particles in matrix of fine $\alpha_2+\gamma$
16	S.T. + 800°C/24hrs/AC	> 12	189	Coarse α_2 + γ mixture
3	S.T. + 800°C/8hrs/AC	> 12	188	Acicular α_2 in fine α_2 + γ matrix
16	1345°C/1hr/AC (S.T.)	> 12	182	Coarse α_2 + γ mixture
11	S.T. + 800°C/24hrs/AC	> 12	174	Coarse α_2 + γ mixture
11	1300°C/1hr/AC (S.T.)	> 12	175	Coarse α_2 + γ mixture
8A	1175°C/2hrs/AC (S.T.)	12	194	Coarse acicular α_2 in β matrix
12	S.T. + 800°C/8hrs/AC	10	257	Coarse α_2 particles in matrix of $\alpha_2 + \gamma$
17	S.T. + 800°C/24hrs/AC	9	187	Planar γ in α_2
5A	1200°C/2hrs/AC (S.T.)	8.4	232	Acicular α_2
25	S.T. + 800°C/8hrs/AC	8.2	186	Planar γ in α_2
2	S.T. + 800°C/8hrs/AC	8.1	177	"
5A	S.T. + 800°C/8hrs/AC	8	178	"
1	S.T. + 800°C/8hrs/AC	8	175	"
1	1160°C/2hrs/AC (S.T.)	6.5	164	Single phase α_2
12	1160°C/2hrs/AC (S.T.)	4	167	Single phase α_2
25	1250°C/2hrs/AC (S.T.	3	170	"
0	S.T. + 800°C/8hrs	9.1	195	Planar γ in α_2
0	S.T.	6.4	155	Single phase α_2

TABLE V

EFFECTS OF ALLOYING ADDITIONS ON ESTIMATED FRACTURE TOUGHNESS AND FLOW STRESS (8% STRAIN)

Alloy Designation	Alloying Addition and Condition	K_c (ksi$\sqrt{in}$)	Alloy Designation	Alloying Addition and Condition	σ (ksi)
Substituting Mo or V for Nb					
4	3% Mo, aged	> 12	4	3% Mo, aged	196
3	1.5% Mo, aged	> 12	3	1.5% Mo, aged	188
2	4.5% V, aged	8.1	2	4.5% V, aged	177
1	2.3% V, aged	8.0	1	2.3% V, aged	175
1	2.3% V, S.T.	6.5	1	2.3% V, S.T.	164
Substituting Ni or Cr for Al					
8A	1% Cr, aged	> 12	5A	1% Ni, S.T.	232
8A	1% Cr, S.T.	12	8A	1% Cr, aged	215
5A	1% Ni, S.T.	8.4	8A	1% Cr, S.T.	194
5A	1% Ni, aged	8.0	5A	1% Ni, aged	178
Substituting Zr for Ti					
11	10% Zr, aged	> 12	10	5% Zr, aged	256
11	10% Zr, S.T.	> 12	11	10% Zr, S.T.	175
			11	10% Zr, aged	174
Substituting Cu or Sn for Al					
12	1.3% Cu, aged	10	12	1.3% Cu, aged	257
17	1.0% Sn, aged	9	17	1.0% Sn, aged	187
12	1.3% Cu, S.T.	4	12	1.3% Cu, S.T.	167
Varying Al Content					
16	45% Al, aged	> 12	16	45% Al, aged	184
16	45% Al, S.T.	> 12	25	42.5% Al, aged	186
25	42.5% Al, aged	8.2	16	45% Al, S.T.	182
25	42.5% Al, S.T.	3	25	42.5% Al, S.T.	170
Base Alloy					
0	Aged	9.1	0	Aged	195
0	S.T.	6.4	0	S.T.	155

TABLE VI

ROOM TEMPERATURE TENSILE TESTS

Alloy Designation	Treatment	Strain Rate(sec^{-1})	Plastic Strain(%)	Fracture Stress(psi)
0	1175°C/1hr/WQ (S.T.)	4.5×10^{-4}	0	26,100
0	S.T. + 800°C/4hrs	4.5×10^{-4}	0	51,200*
1	1175°C/2hrs/AC(S.T.)	2.2×10^{-4}	0	19,000*
1	S.T. + 800°C/4hrs	2.2×10^{-4}	0.15	102,600
1	S.T. + 800°C/24hrs	2.2×10^{-4}	0	38,000
3	1175°C/2hrs/AC(S.T.)	2.2×10^{-4}	0	53,000*
3	S.T. + 800°C/8hrs	2.2×10^{-4}	0	57,800*
4	1175°C/2hrs/AC(S.T.)	2.2×10^{-4}	0	53,000*
4	S.T. + 800°C/8hrs	2.2×10^{-4}	0	37,000*
8A	1175°C/1hr/AC(S.T.)	2.2×10^{-4}	0	101,800
8A	S.T. + 800°C/16hrs	2.2×10^{-4}	0	73,000*
11	1285°C/1hr/AC(S.T.)	2.2×10^{-4}	0	55,200
11	S.T. + 800°C/8hrs	2.2×10^{-4}	0	28,900*
23	S.T. + 800°C/48hrs	2.2×10^{-4}	0	46,000
23	S.T. + 800°C/96hrs	2.2×10^{-4}	0	81,000
26	1250°C/½hr/AC(S.T.)	2.2×10^{-4}	0	22,000
26	S.T. + 800°C/8hrs	2.2×10^{-4}	0	37,000
26	S.T. + 800°C/48hrs	2.2×10^{-4}	0.22	95,000*
26	S.T. + 800°C/96hrs	2.2×10^{-4}	0	95,000
6219-A	As extruded	4.5×10^{-4}	0	34,200*
6219-A	1175°C/1hr/AC(S.T.)	4.5×10^{-4}	0	30,900*
6219-A	S.T. + 800°C/4hrs	2.2×10^{-4}	0	53,500*

* failed in sample shoulder

TABLE VII

1400°F (760°C) TENSILE TESTS

Alloy Designation	Treatment	Strain Rate(sec^{-1})	Fracture Stress (psi)	Yield Stress (psi)	Ultimate Tensile Stress (psi)	Elongation (%)
0	1175°C/1hr/WQ(S.T.)	2.2×10^{-4}	51,900			
0	S.T. + 800°C/8hrs	3.3×10^{-4}	38,400			
1	1175°C/2hrs/AC(S.T.)	2.2×10^{-4}	18,400			
1	S.T. + 800°C/8hrs	3.3×10^{-4}	43,300			
3	S.T. + 800°C/8hrs	2.2×10^{-4}	67,800			
4	S.T. + 800°C/8hrs	2.2×10^{-4}	59,400			
8A	1175°C/1hr/AC(S.T.)	3.3×10^{-4}		54,900	73,200	2
8A	S.T. + 800°C/8hrs	3.3×10^{-4}		95,900	105,900	1.5
11	1285°C/1hr/AC(S.T.)	2.2×10^{-4}	48,400			
11	S.T. + 800°C/8hrs	3.3×10^{-4}	51,800			
23	1250°C/1hr/AC(S.T.)	2.2×10^{-4}	22,600			
23	S.T. + 800°C/8hrs	2.2×10^{-4}	68,300			
26	1250°C/1hr/AC(S.T.)	2.2×10^{-4}	67,700			
26	S.T. + 800°C/8hrs	2.2×10^{-4}	58,100			

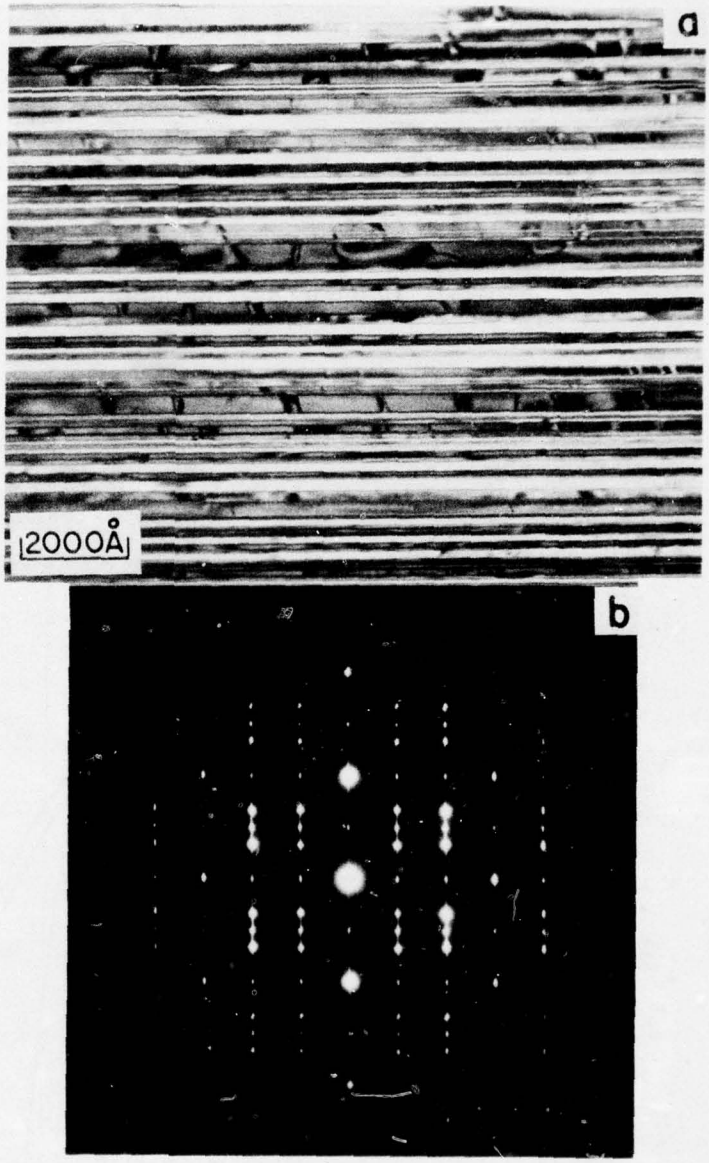

Fig. 1. Transmission electron micrograph (TEM) of Alloy O (Ti-26 wt.pct. Al - 10 wt.pct. Nb) aged at 800°C illustrating planar γ-phase precipitation in α_2 matrix. (a) Bright field image; (b) selected area electron diffraction (SAD) pattern revealing $\{11\bar{2}0\}$ α_2 zone with 2 variants of γ-phase having <110> zone normal.

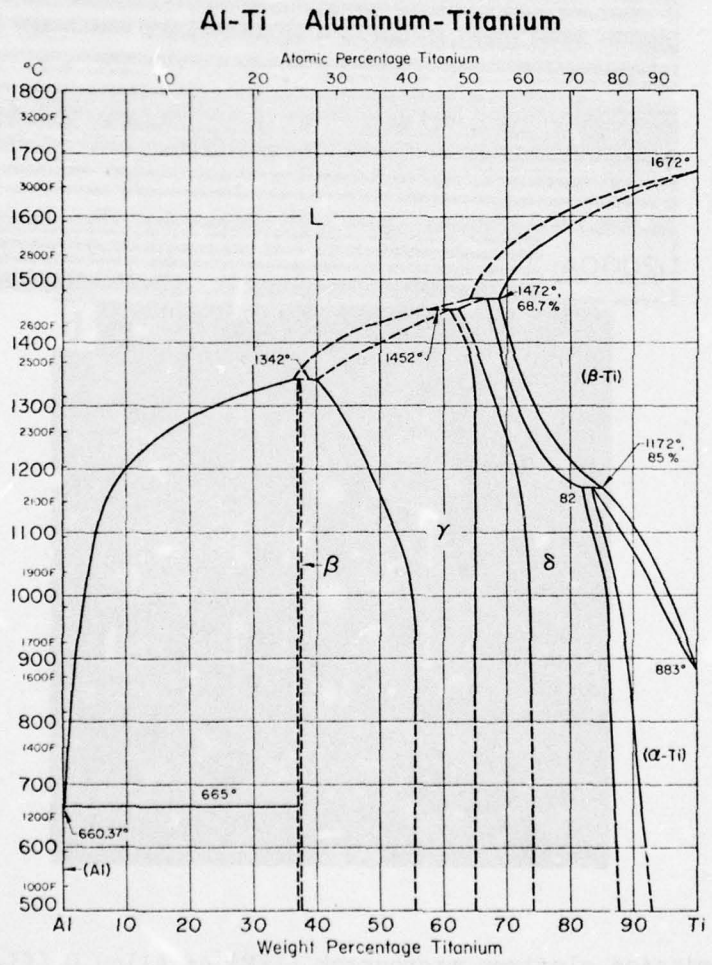

Fig. 2. Al-Ti phase diagram, as published in Metals Handbook.[3]

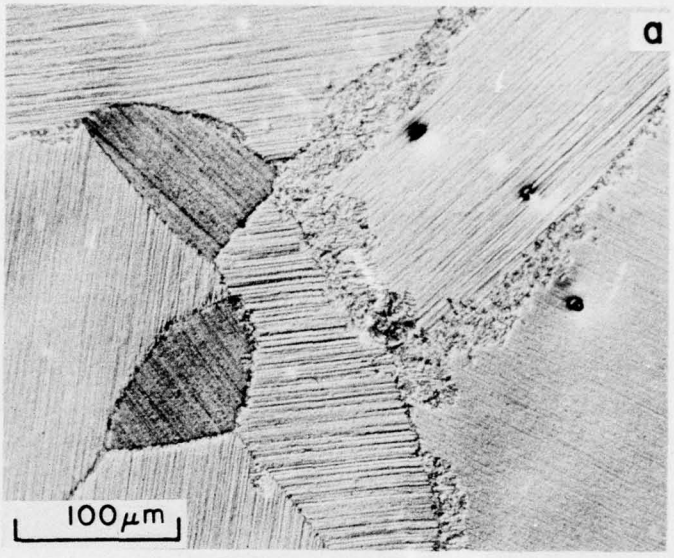

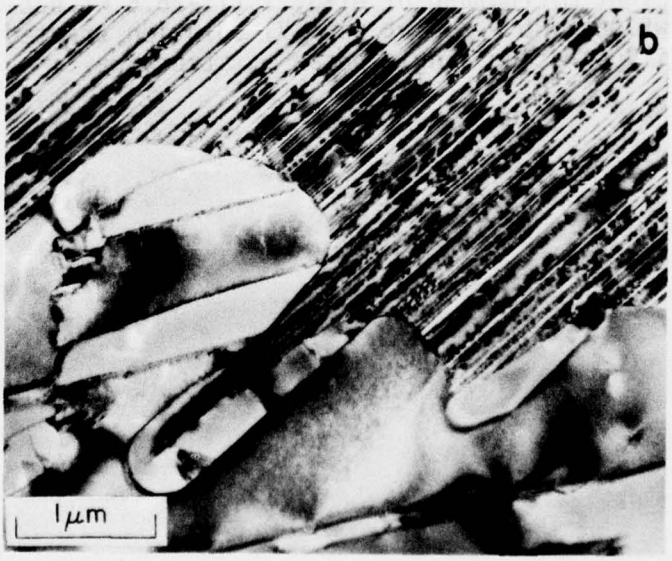

Fig. 3. Cellular reaction, $\alpha_2 \rightarrow \alpha_2 + \gamma$, in Alloy 0 aged at 1000°C. (a) Light micrograph; (b) TEM.

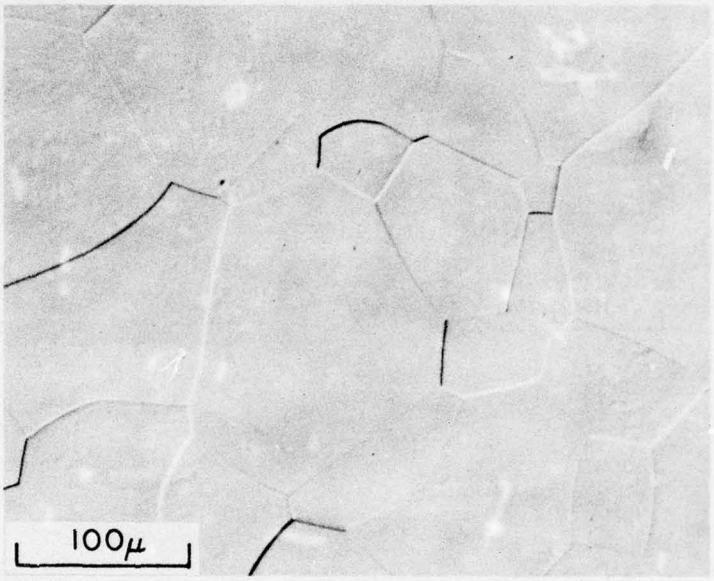

Figure 4. Light micrograph of Alloy 1 (Ti-26.6 wt.pct. Al - 5.3 wt.pct. Nb - 2.4 wt.pct. V) solution treated at 1150°C illustrating single phase α_2 structure.

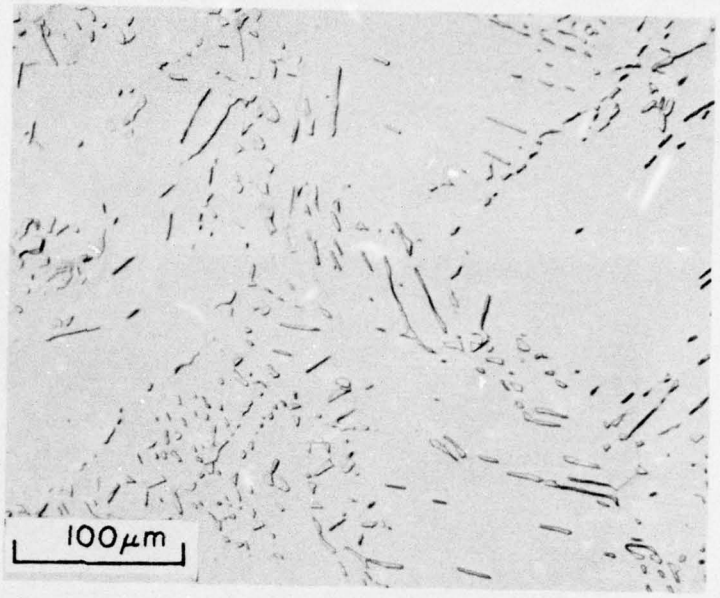

Fig. 5. Light micrograph of Alloy 2 (Ti-27.2 wt.pct. Al - 5.8 wt.pct. V) solution treated at 1250°C illustrating retained β particles in α_2 matrix.

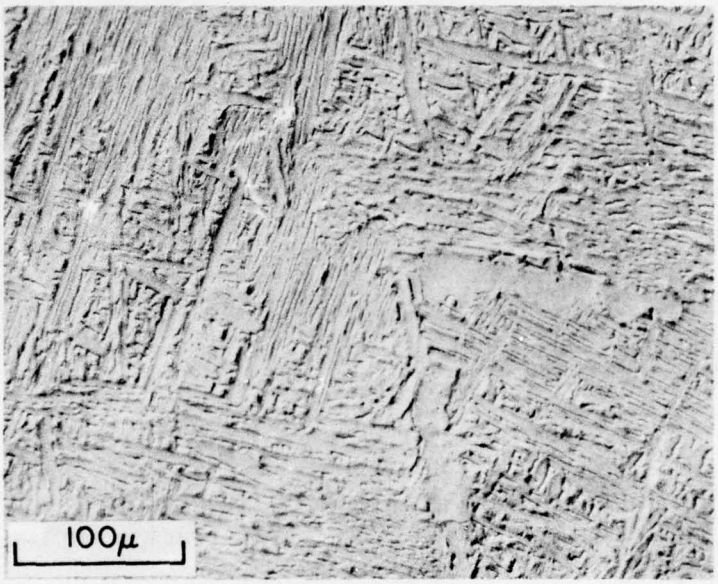

Figure 6. Light micrograph of Alloy 3 (Ti-26.8 wt.pct. Al - 3.6 wt.pct. Mo) solution treated at 1175°C illustrating α_2 laths and retained β_2 structure.

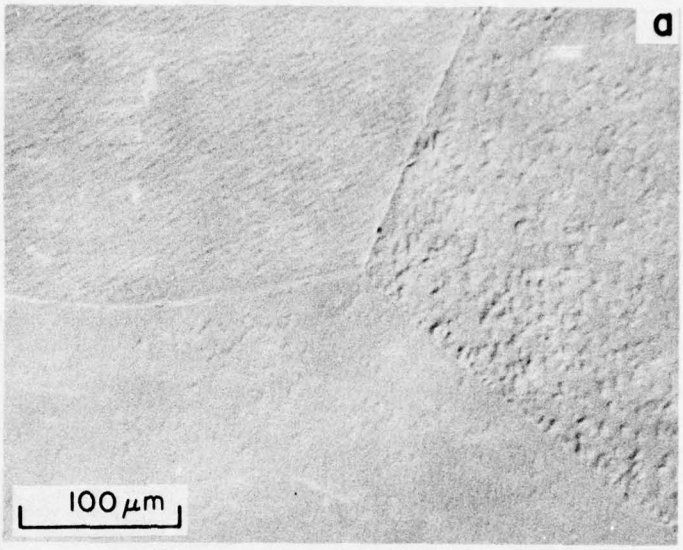

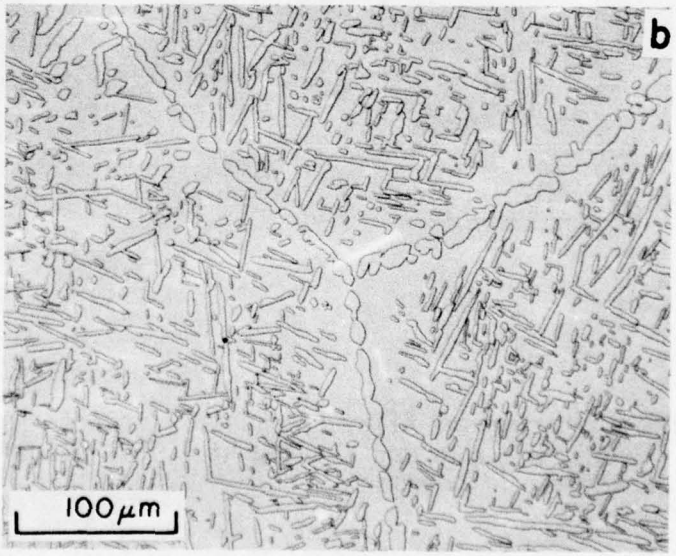

Fig. 7. Light micrographs of Alloy 4 (Ti-26.3 wt.pct Al - 7.0 wt.pct. Mo) (a) solution treated at 1300°C: 100% β_2; (b) solution treated at 1200°C: α_2 particles in β_2 matrix.

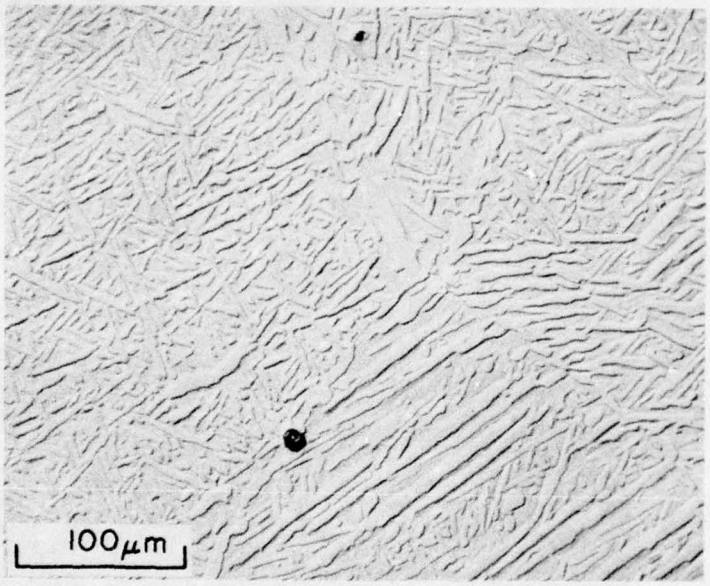

Fig. 8. Light micrograph of Alloy 5A (Ti-25.1 wt.pct. Al - 1.4 wt.pct. Ni - 10 wt.pct. Nb) solution treated at 1175°C illustrating lath-like α_2 particles in β_2 matrix.

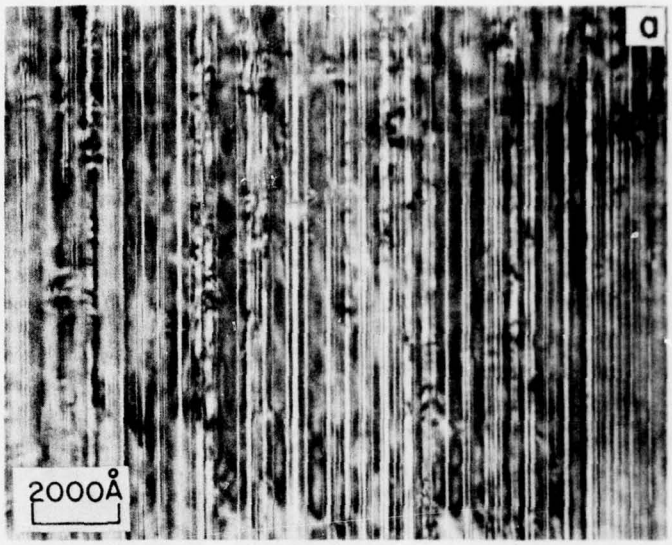

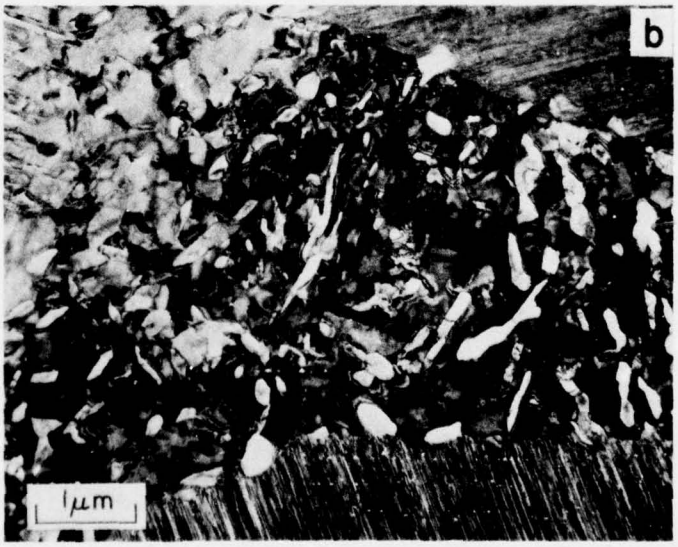

Fig. 9. TEM of Alloy 5A aged at 800°C. (a) Planar γ-phase precipitates in α_2 laths; (b) decomposed β_2 region.

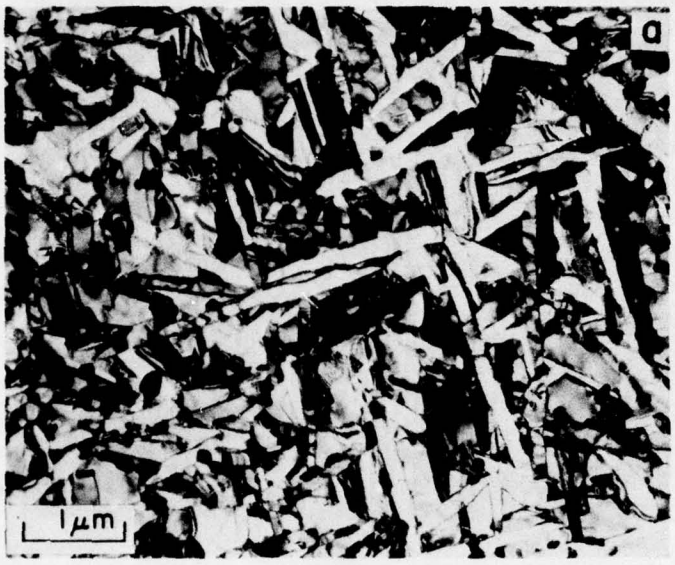

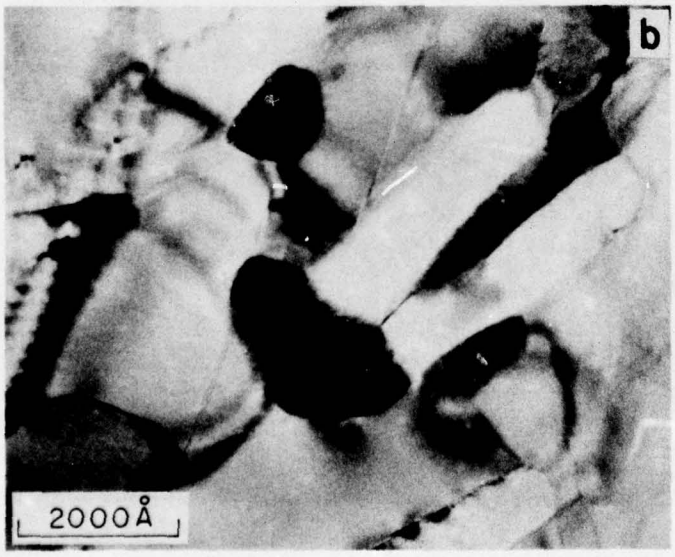

Fig. 10. TEM of Alloy 7 (Ti-18.1 wt.pct. Al - 13.1 wt.pct. Ni - 9.3 wt.pct. Nb) aged at 800°C. (a) Lath-like α_2 precipitates; (b) faulted Ti_2Ni particles.

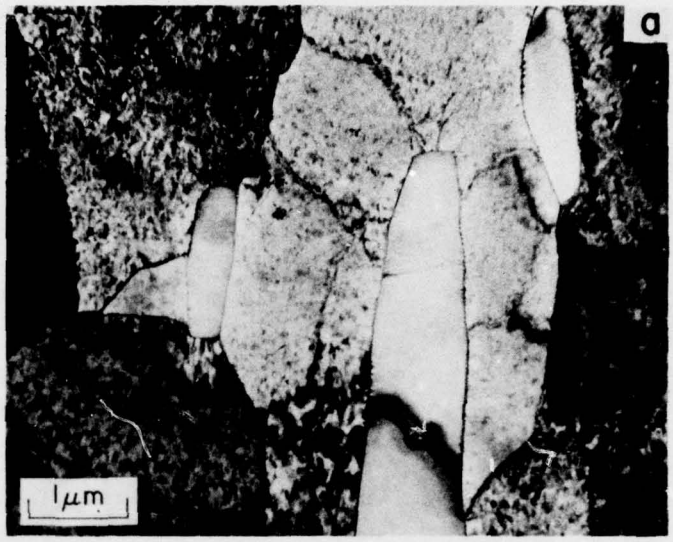

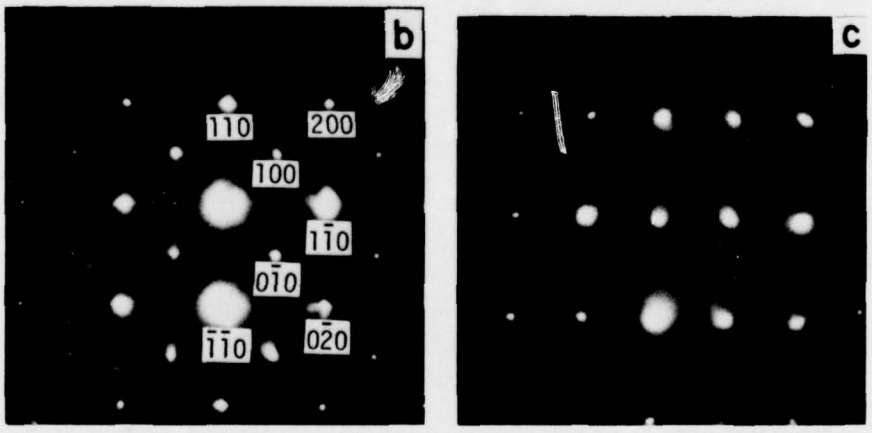

Fig. 11. TEM of Alloy 8A (Ti-25.2 wt.pct. Al - 1.2 wt.pct. Cr - 10 wt.pct. Nb) solution treated at 1175°C. (a) Elongated β_2 particles in α_2 matrix; (b) SAD of [001] β_2 zone illustrating presence of superlattice reflections; (c) SAD of [$1\bar{1}0$] β_2 zone revealing ω-phase reflections.

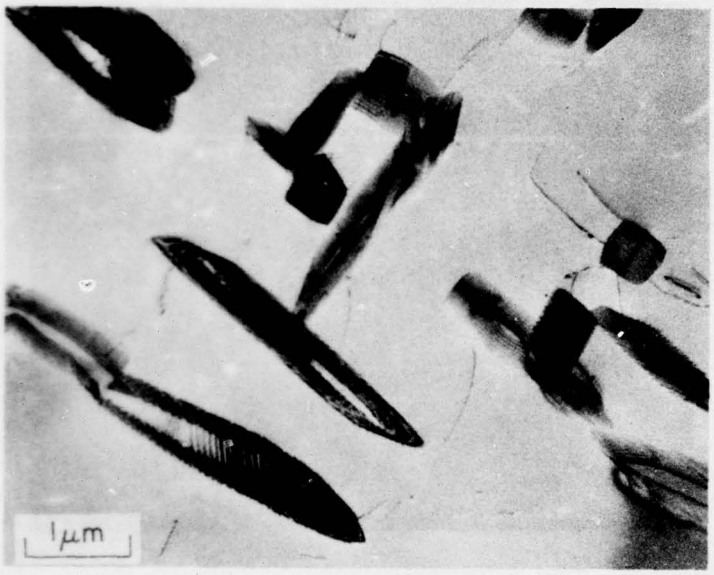

Fig. 12. TEM of Alloy 8 aged at 800°C illustrating α_2 particles in β_2 matrix.

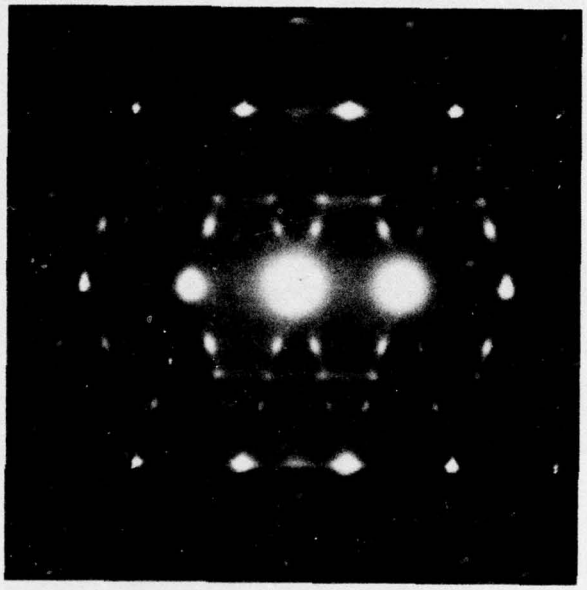

Figure 13. SAD pattern of Alloy 10 (Ti-24.7 wt.pct. Al - 9.6 wt.pct. Nb - 10.4 wt.pct. Zr) quenched from 1300°C, illustrating omega reflections in [113] ordered β zone.

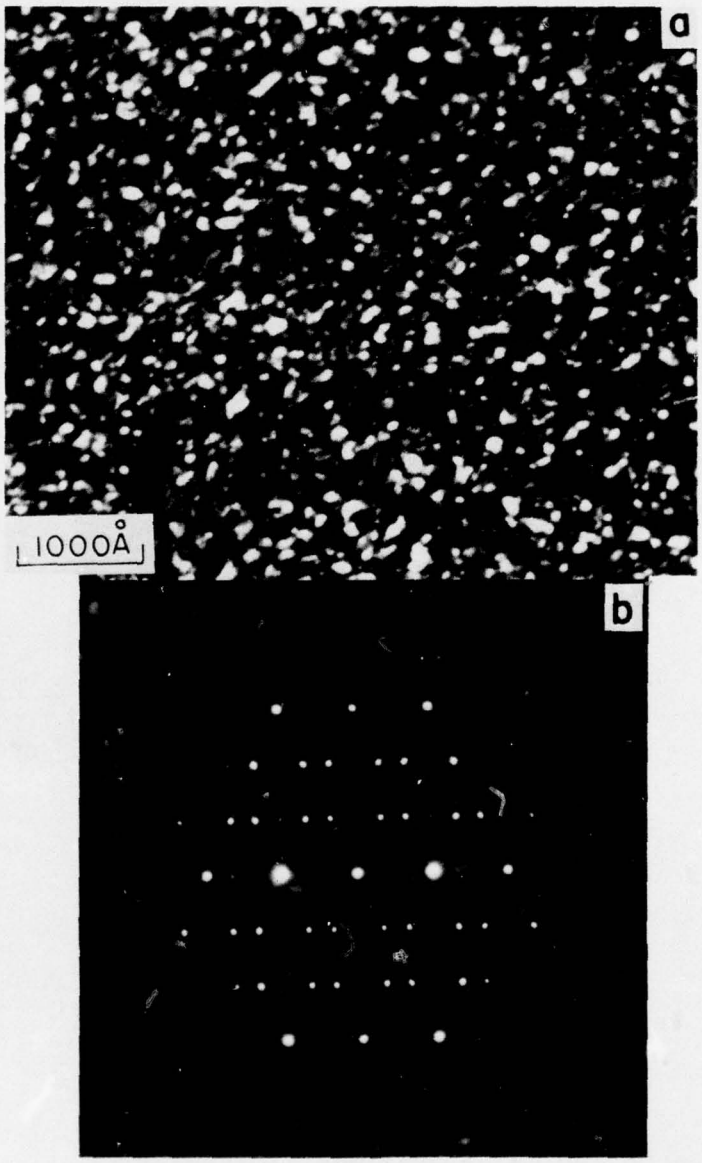

Figure 14. Omega phase precipitation in ordered β matrix in Alloy 10 aged at 600°C for 2 hours. (a) TEM, (b) SAD pattern of [210] ordered β-zone with 2 [$\bar{1}\bar{1}26$] ω-phase zones.

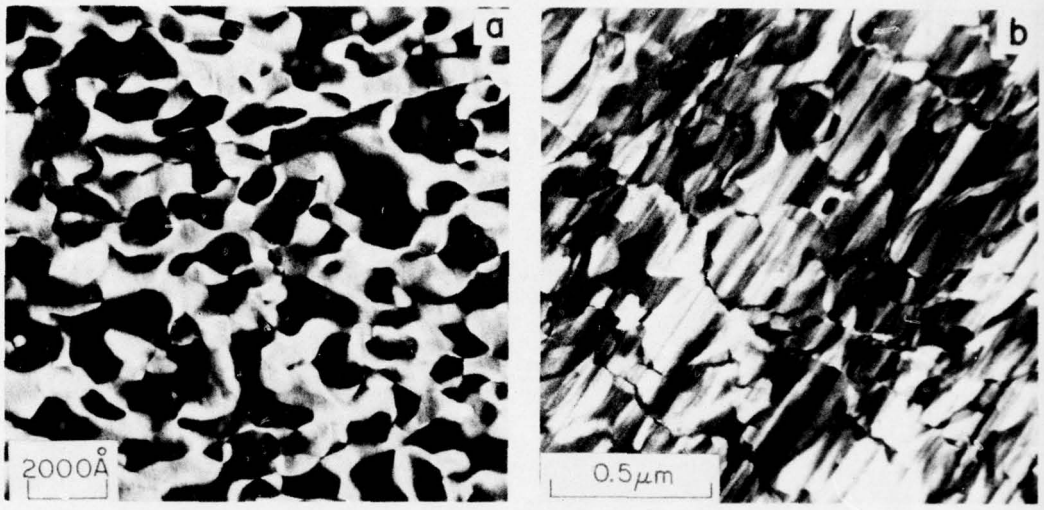

Fig. 15. Dark field TEM of Alloy 0 illustrating ordered domains, $(10\bar{1}1)\ \alpha_2$ reflection operating. (a) As solution treated; (b) solution treated and aged at 800°C for 8 hours.

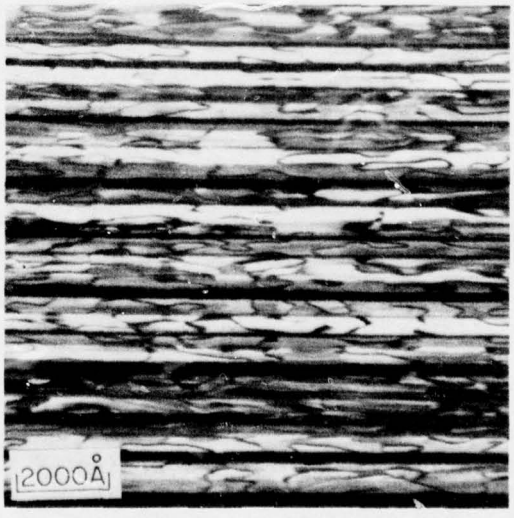

Fig. 16. Dark field TEM of Alloy 11 solution treated and aged at 800°C for 4 hours, illustrating ordered domains. $(10\bar{1}1)\ \alpha_2$ reflection operating.

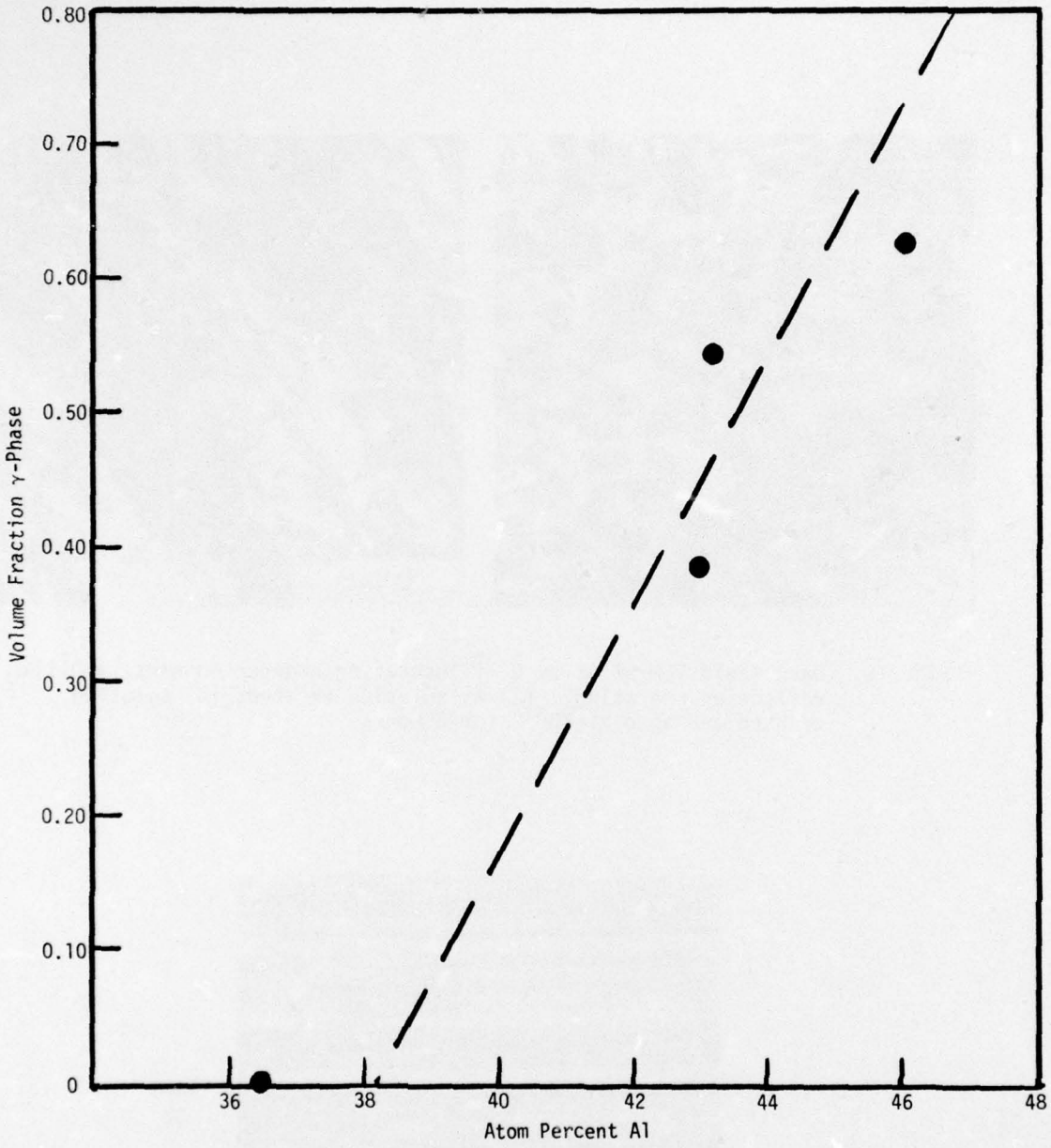

Fig. 17. Volume fraction γ-phase as a function of Al content in Ti alloys containing 4.5 at.pct. Nb aged 24 hours at 800°C. Dashed line is that predicted by Ti-Al phase diagram.

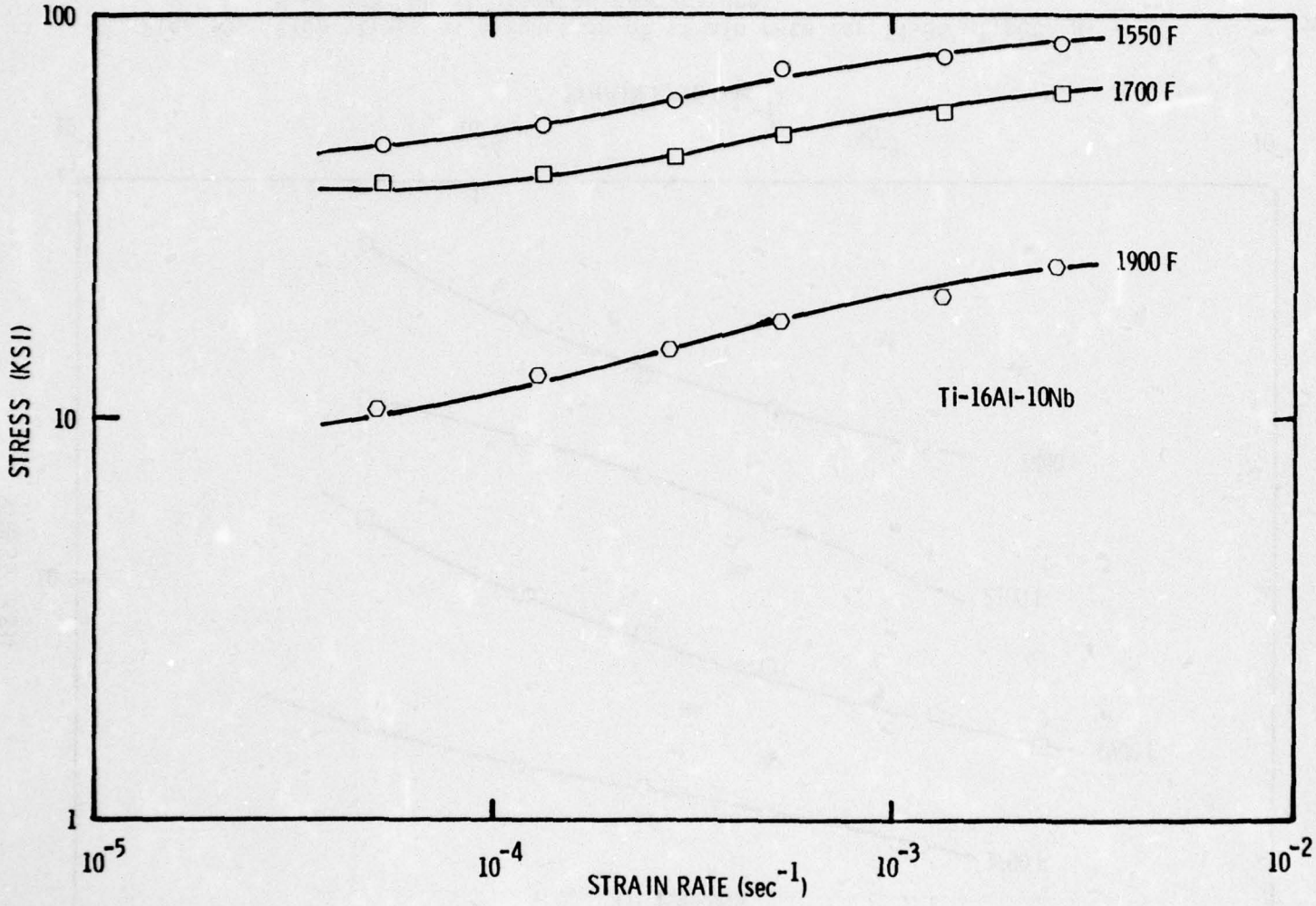

Fig. 18. Flow stress as a function of strain rate for Ti-16 wt.pct. Al - 10 wt.pct. Nb at elevated temperatures.

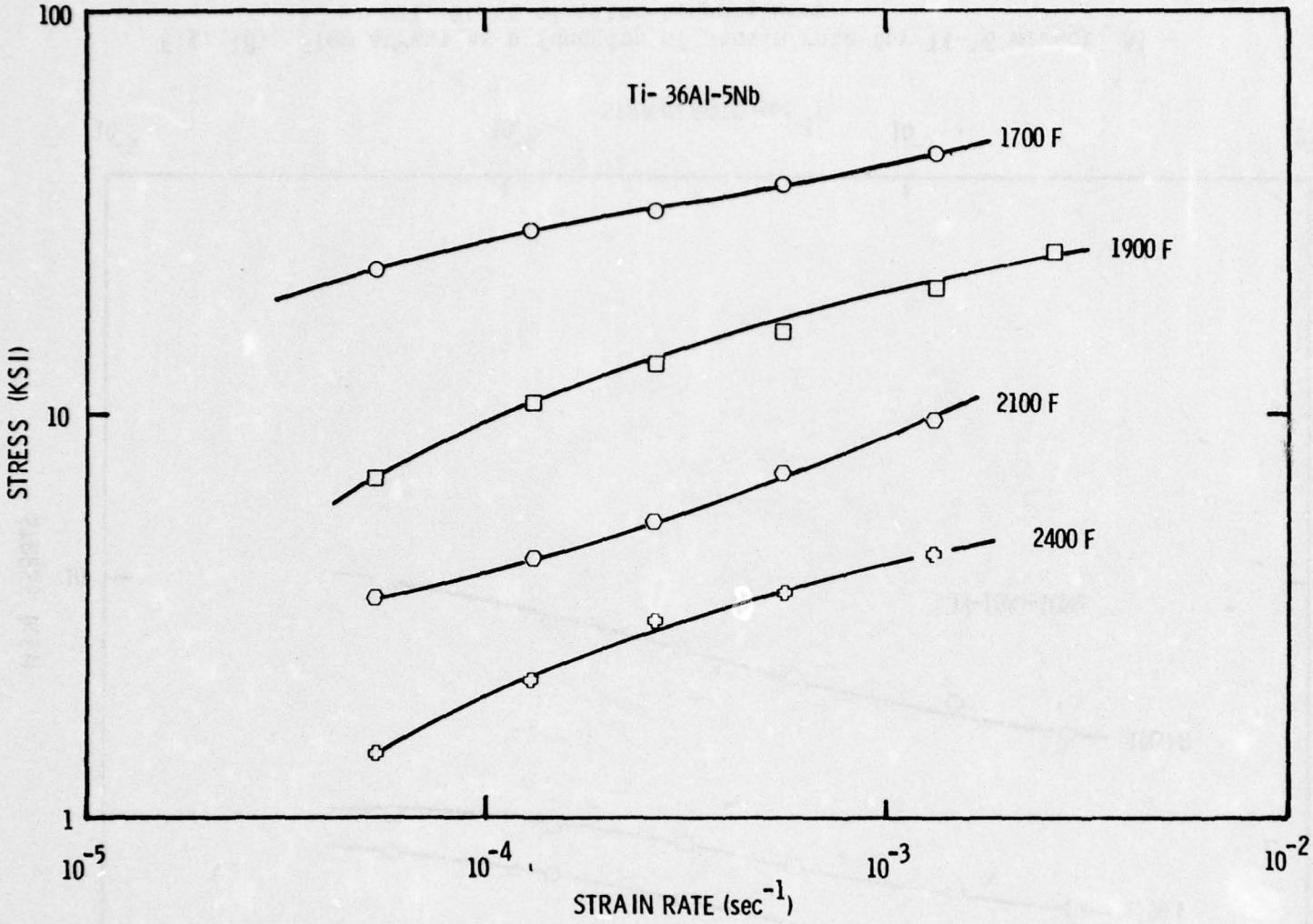

Fig. 19. Flow stress as a function of strain rate for Ti-36 wt.pct. Al - 5 wt.pct. Nb at elevated temperatures.

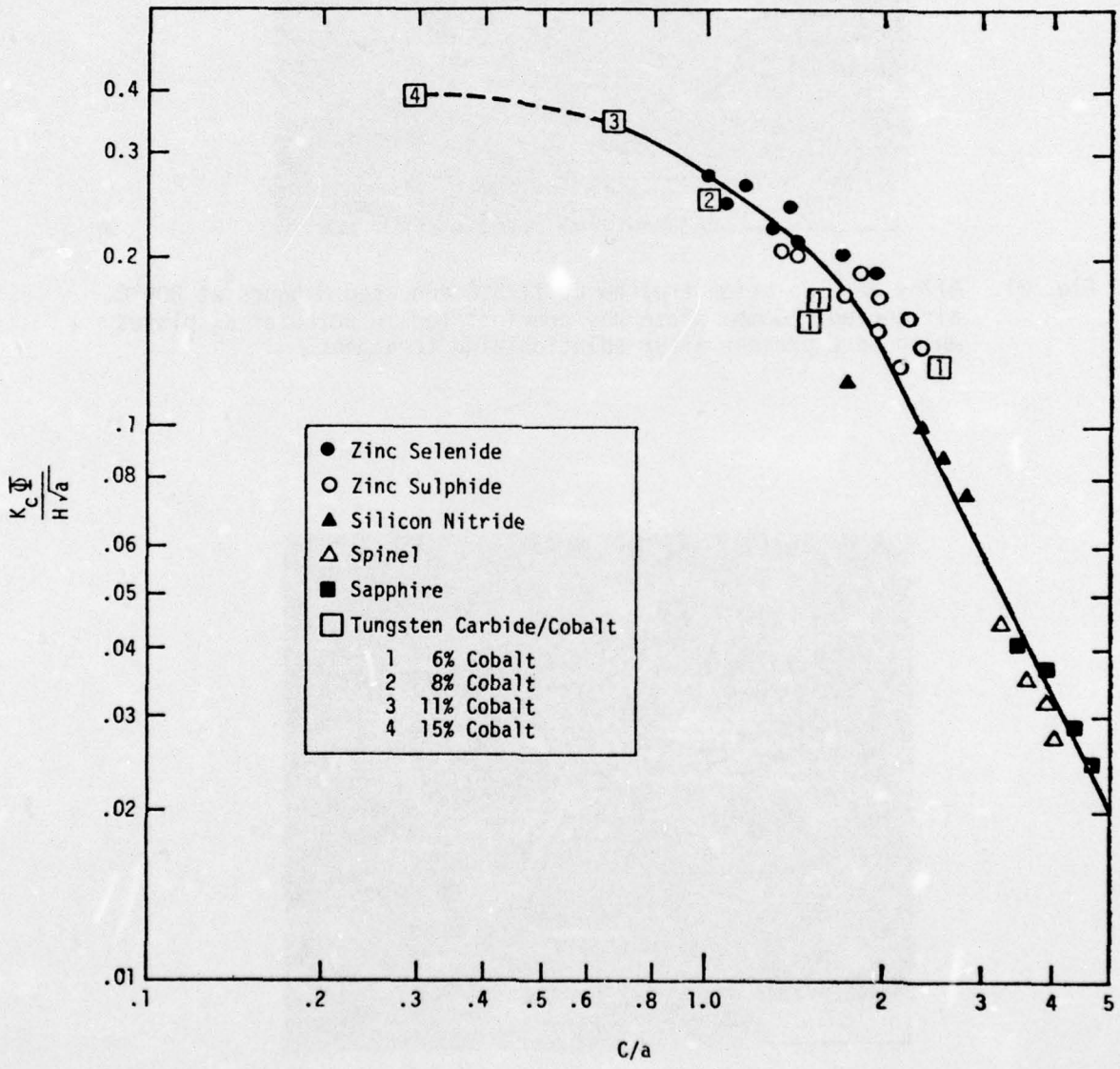

Fig. 20. The normalized fracture toughness, $K_c\phi/H\sqrt{a}$, as a function of the normalized crack length, C.

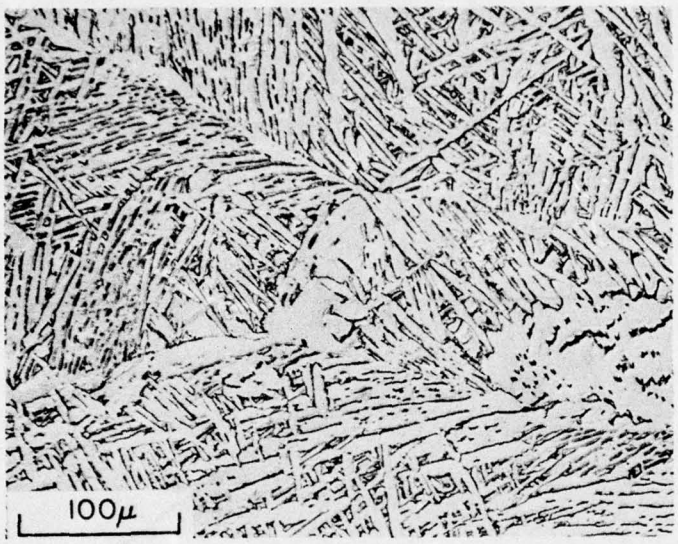

Fig. 21. Alloy 8A. Solution treated at 1175°C and aged 8 hours at 800°C, air cooled. Gamma phase has precipitated in acicular α_2 plates which were present after solutionizing treatment.

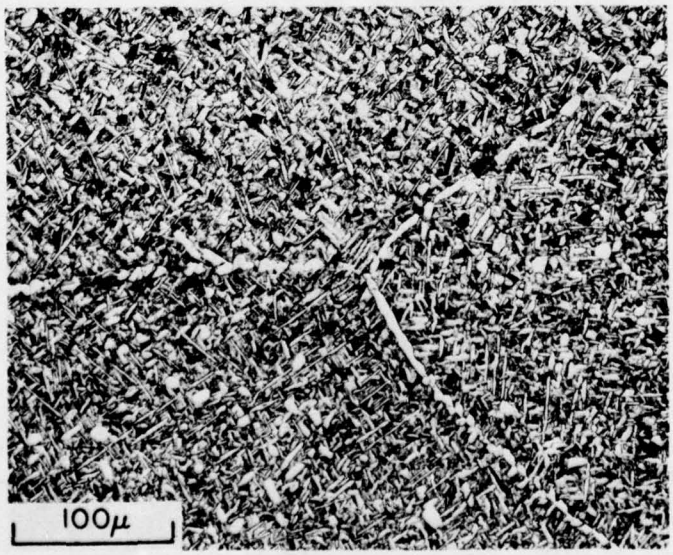

Fig. 22. Alloy 4. Solution treated at 1175°C and aged 8 hours at 800°C, air cooled. Beta matrix has decomposed to $\alpha_2 + \gamma$ phases during aging treatment. Coarse α_2 particles were present after solutionizing treatment.

Fig. 23. Alloy 16. Solution treated at 1345°C and aged 24 hours at 800°C, air cool. The coarse mixture of α_2 and γ phases was unaltered by aging treatment.

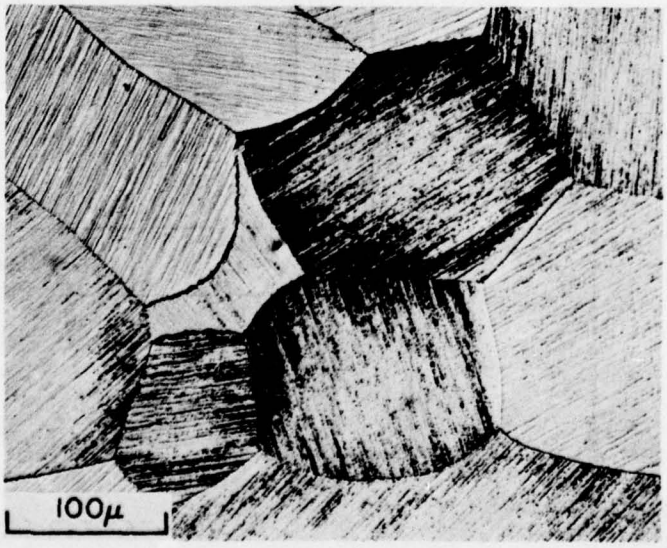

Fig. 24. Alloy 2. Solution treated at 1160°C and aged 8 hours at 800°C, air cool. The fine planar γ-phase precipitation in α_2 matrix is typical of base alloy microstructure.

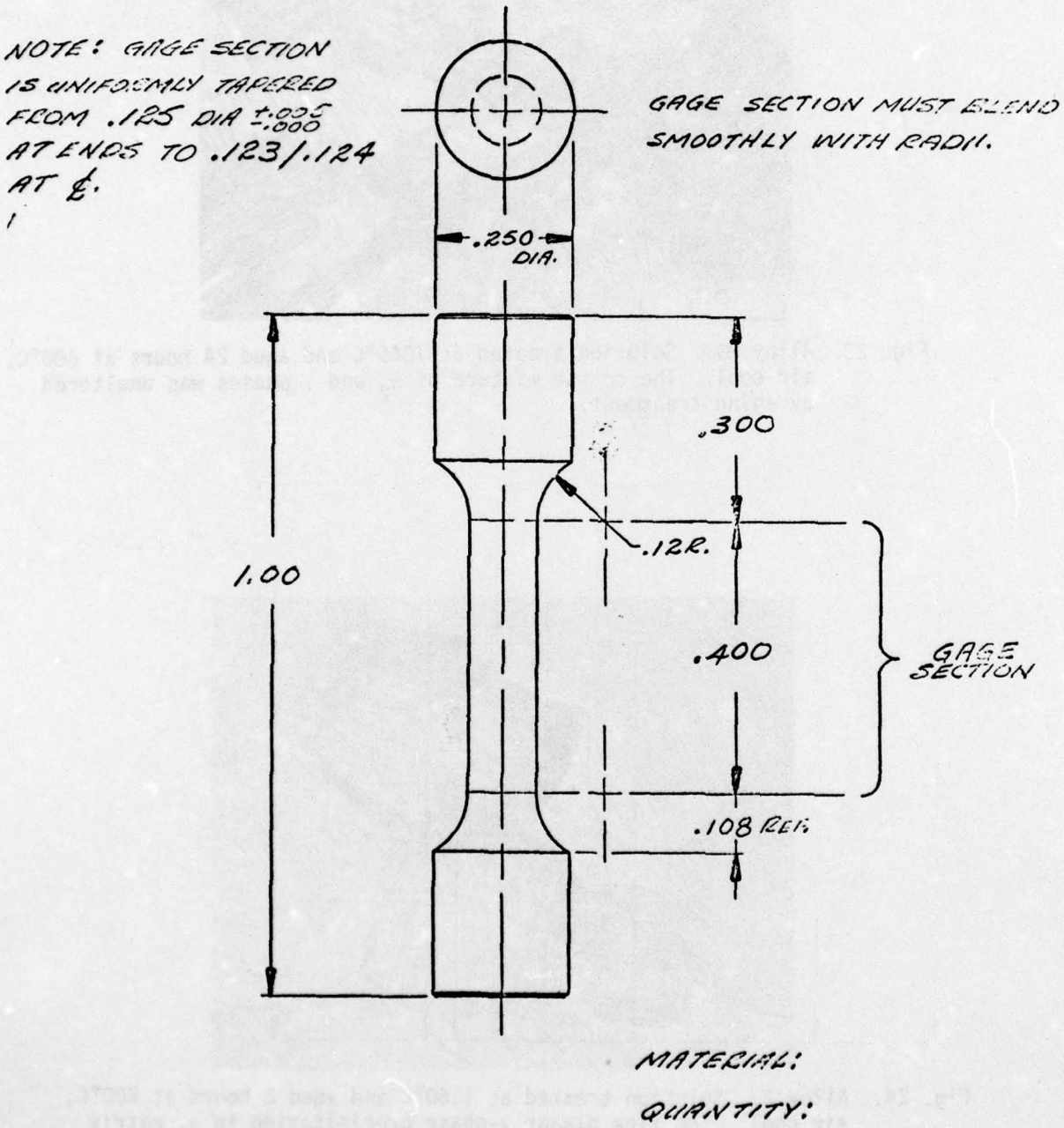

Fig. 25. Tensile sample configuration.

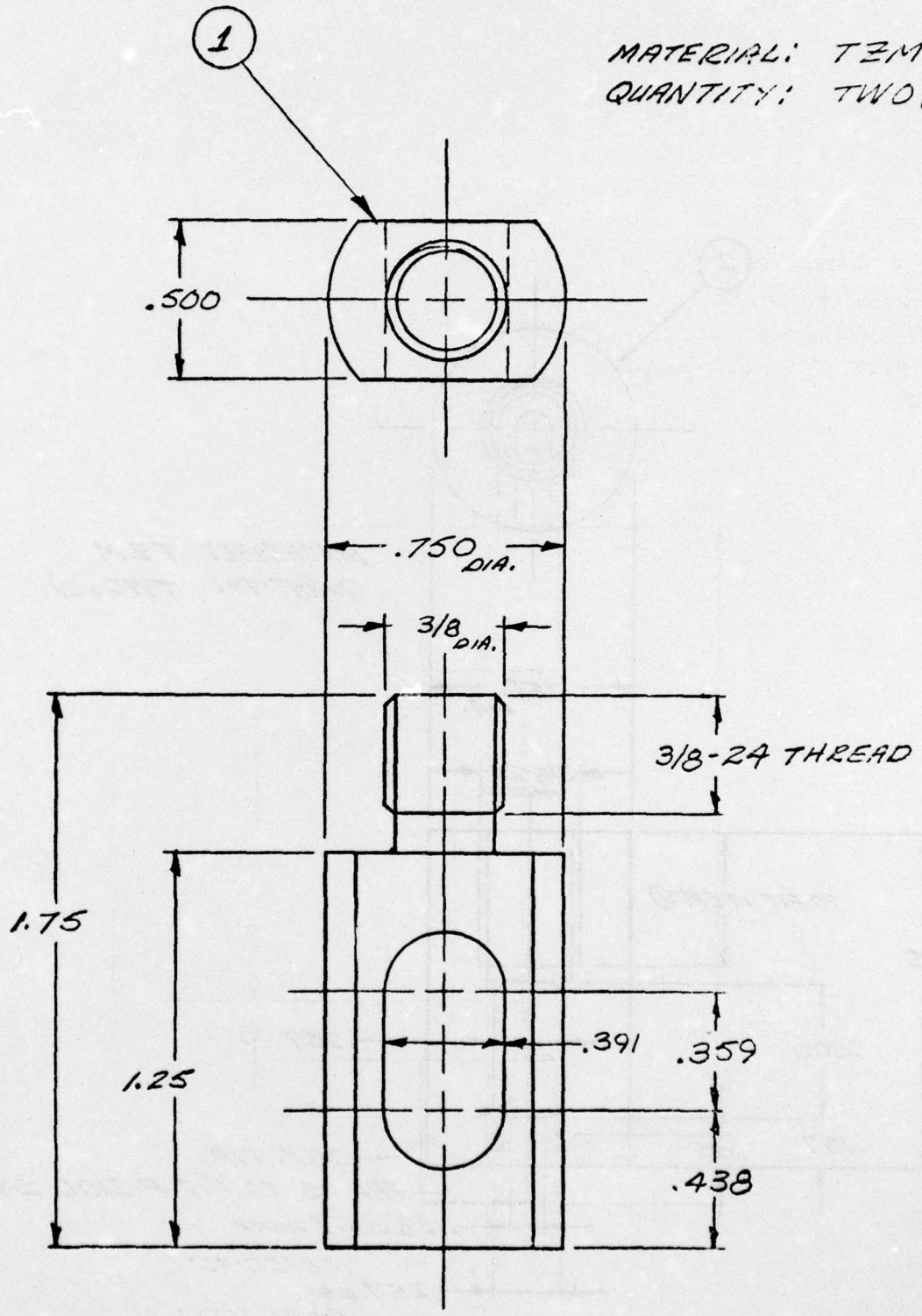

Fig. 26(a). Tensile sample grip configuration.

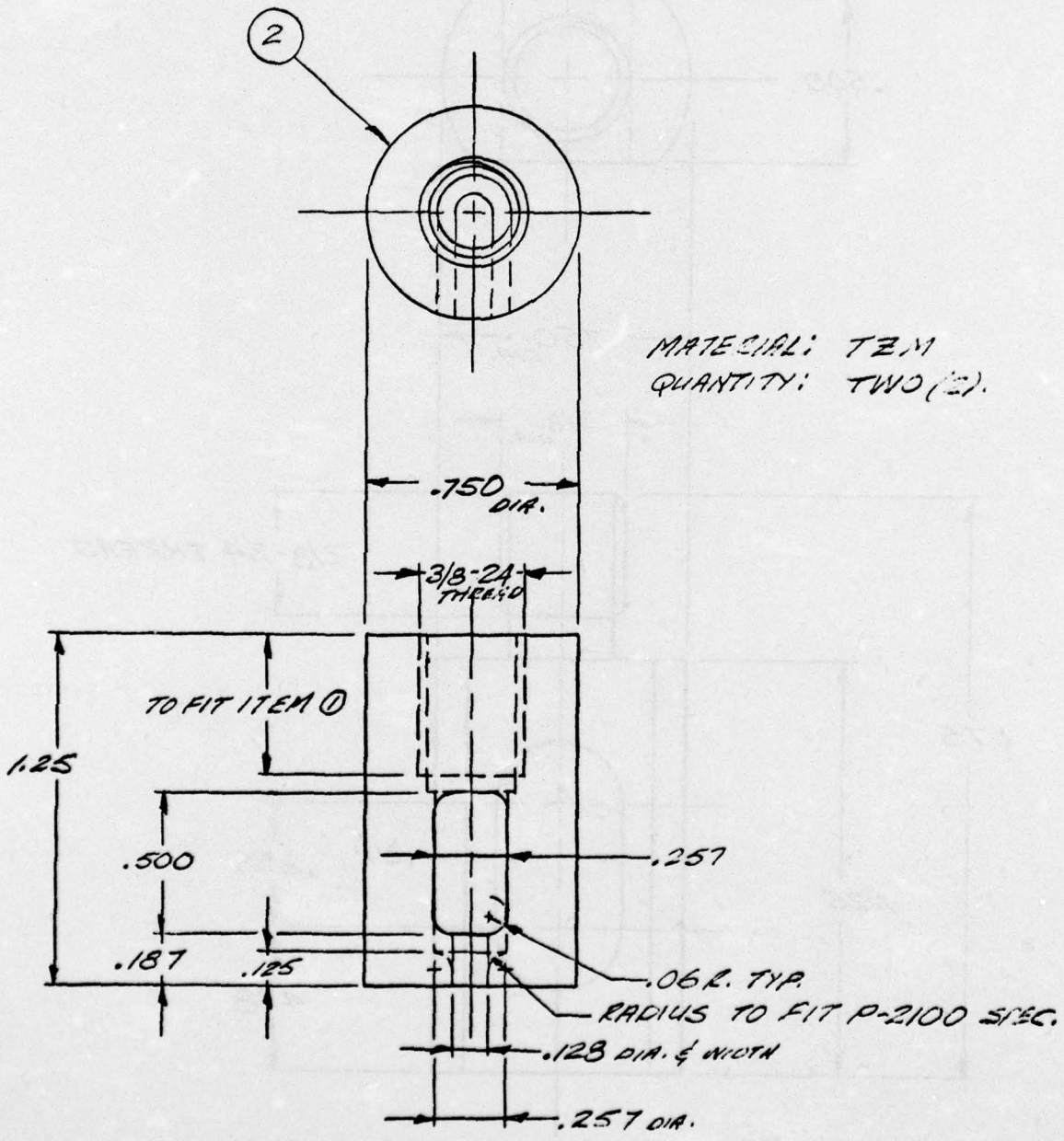

Fig. 26(b). Tensile sample grip configuration.

Figure 27. Scanning electron micrograph (SEM) of fracture surface of solution treated Alloy 0 tensile sample.

Figure 28. SEM of fracture surface of aged Alloy 0 tensile sample.

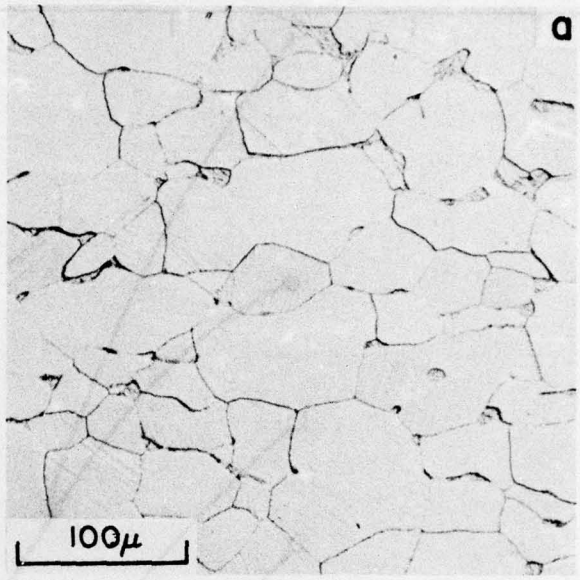

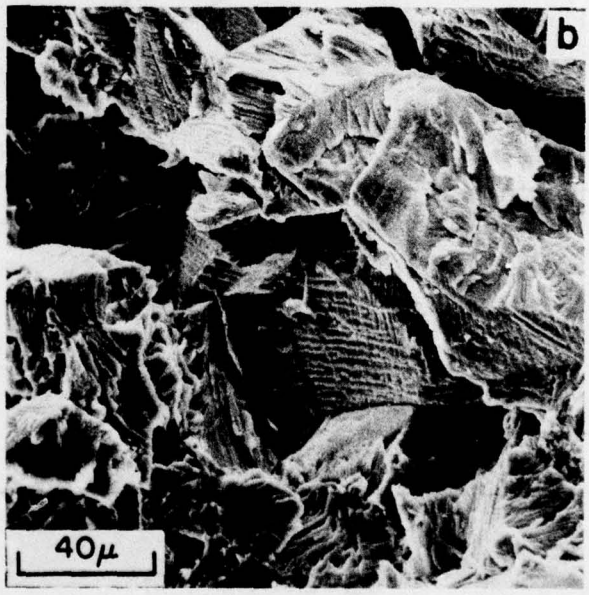

Figure 29. Alloy 1. Hot pressed at 1250°C, solutionized and aged 4 hours at 800°C. (a) light micrograph, (b) SEM of fracture surface.

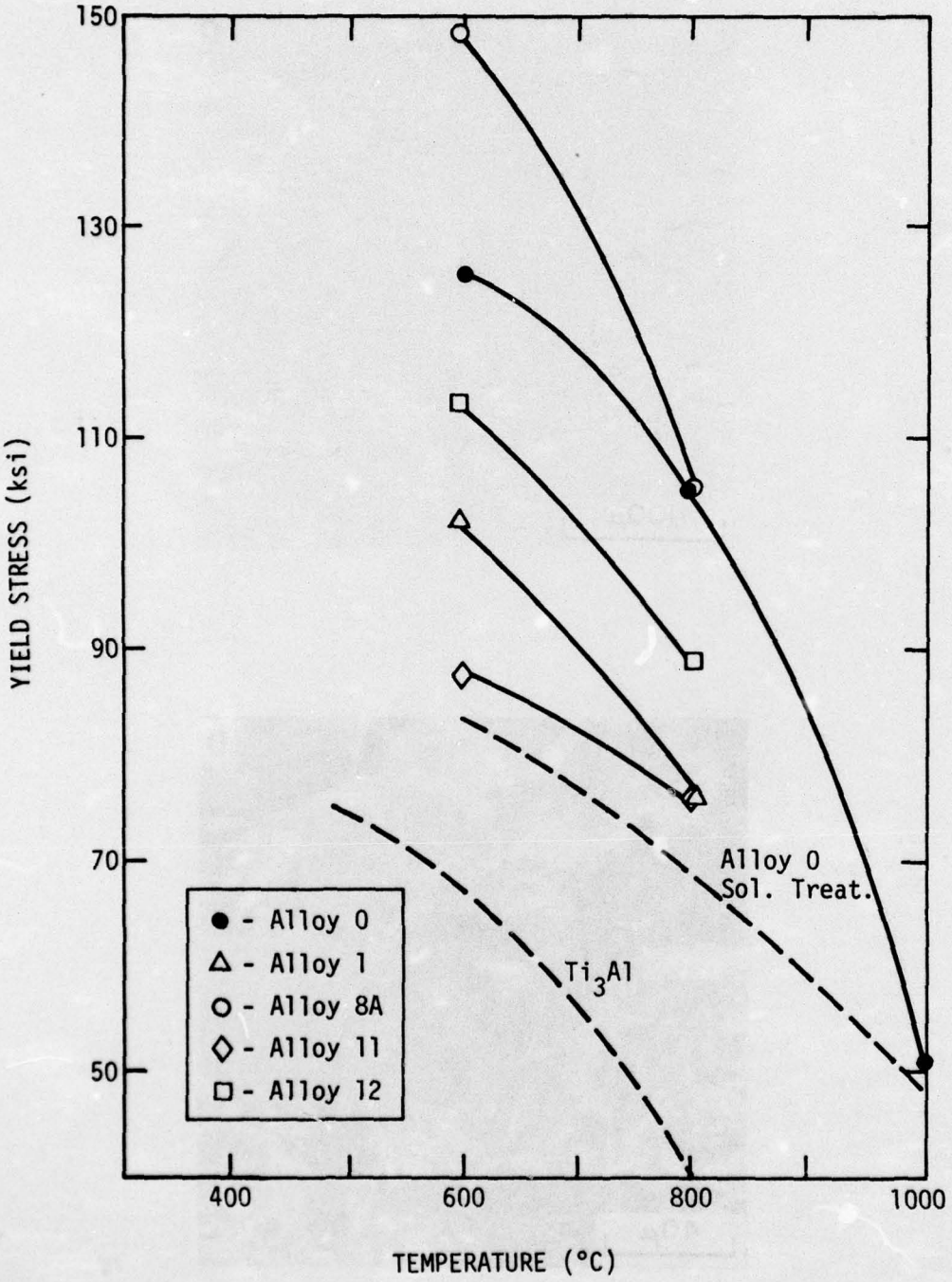

Fig. 30. Compression yield strength as a function of test temperature for five alloys solutionized and aged at 800°C.

☆ U. S. GOVERNMENT PRINTING OFFICE: 1976 — 657-630/1044